




# Effectiveness of vaccination, travel load, and facemask use control strategies for controlling COVID Delta variant: the case of Sydney Metropolitan Area

Maliheh Tabasi<sup>1</sup> · Ali Najmi<sup>1</sup> · Eric J. Miller<sup>2</sup> · C. Raina MacIntyre<sup>3,4</sup> · Taha H. Rashidi<sup>1</sup> 

Accepted: 6 February 2024  
© The Author(s) 2024

## Abstract

The Delta variant of SARS-CoV-2, specifically identified as B.1.617.2, is responsible for the severe outbreaks witnessed globally, including in various countries and cities, with Sydney Greater Metropolitan Area (Sydney GMA) being no exception. According to scientific studies, the Delta strain exhibits increased contagion and leads to a higher incidence of vaccine breakthrough cases, posing significant challenges to pandemic control efforts. In this study, we explore the efficacy of three fundamental control strategies—namely, vaccination rates, adherence to facemask usage, and the management of travel loads—in mitigating the spread of the disease and, consequently, eliminating the Delta variant pandemic in Sydney GMA. We employ an agent-based disease spread model to thoroughly investigate these strategies. Moreover, factorial MANOVA is utilised to assess the significance of variations in the impact of diverse compliance levels with the aforementioned control strategies on various attributes of the pandemic. As complete lockdowns and stringent travel regulations have the potential to induce physical and mental distress in individuals and economic crises for countries, our study examines the interactive effects of implementing control strategies to mitigate the necessity for a full lockdown. The simulation results suggest that suppressing a pandemic with similar characteristics to Delta variant of COVID is feasible with a vaccination rate of 80% or higher, as long as travel load and activity participation are maintained at pre-COVID levels. Alternatively, a more realistic and attainable combination of control measures—a vaccination rate of 60%, a facemask usage level of 60%, and a 50% compliance level for social distancing—demonstrates comparable efficacy, leading to effective pandemic control. Notably, the vaccination rate emerges as a more potent control strategy compared to others in the elimination of the disease within society.

**Keywords** Delta pandemic · Vaccination rate · Disease spread agent-based model · Control strategies

## Introduction

In 2023, while not as severe as the years 2020 to 2022, the world still contends with a persistent pandemic brought about by the severe acute respiratory syndrome coronavirus 2 (SARS-CoV-2), which initially emerged in Wuhan, China, in December 2019. Since that time, countries worldwide have implemented various control strategies to curb the spread of the disease, including case isolation, social distancing, facemask usage, full lockdowns, teleworking, school closures, and more. While these control measures proved largely successful in managing the pandemic induced by the original, Alpha, and Beta variants of the coronavirus, the challenge escalated with the emergence of the Delta variant of COVID-19. Controlling the pandemic, primarily driven by the Delta variant, posed heightened difficulties despite the prior success of these strategies. Although the outbreak caused by the Delta variant has now subsided, it would be beneficial to examine the characteristics of this virus and investigate which combination of control strategies could be efficient according to a disease spread model. This information can be valuable in addressing outbreaks with similar characteristics in the future.

The SARS-CoV-2 Delta variant, originating in India, posed a new global challenge in the latter half of 2021, being approximately 60% more contagious than the original coronavirus strain (Yang and Shaman 2021) and exhibiting a viral load roughly 1000 times greater than the original strain (Li et al. 2021). The control strategies in place proved insufficient in halting the Delta pandemic due to the virus's heightened transmissibility and viral load. Illustrating this challenge, the situation in the Sydney Greater Metropolitan Area (Sydney GMA) serves as a notable example. While the strategies employed in Sydney GMA had significantly curbed the spread and successfully controlled previous strains of the coronavirus, the primary control measure—full lockdown—proved less effective in suppressing the Delta variant-induced pandemic. Consequently, alternative strategies, such as achieving a high vaccination rate, became indispensable in gaining control over the pandemic.

As an adjunct control strategy, the investigation into vaccination merits attention to comprehend its potential in aiding countries to effectively confront and overcome the Delta variant pandemic or future pandemics with similar characteristics. Drawing from studies conducted in Scotland, England, and Canada to assess vaccine efficacy, although vaccination demonstrated effectiveness of up to 90% in reducing non-Delta infections, hospitalisations, and deaths, the occurrence of vaccine breakthrough cases was more prevalent with the Delta variant. The efficiency of vaccination diminished to a range of 79–87% in controlling infections, while its effectiveness in reducing hospitalisations and deaths remained constant (Lopez Bernal et al. 2021; Nasreen et al. 2021; Sheikh et al. 2021). This nuanced understanding of vaccination effectiveness is a pivotal consideration when examining the impact of vaccination rates on gaining control over Delta or analogous pandemics.

Another crucial aspect worth noting is that economic restrictions cannot be sustained indefinitely. Research findings indicate that prolonged implementation of stringent control measures, such as extended periods of full lockdowns, may lead to mental health issues and psychological distress (Hawryluck et al. 2004), as well as physical consequences like muscle loss (Kirwan et al. 2020), affecting both adults and adolescents (Fegert et al. 2020). Consequently, an extended lockdown may not be viable. This paper delves into determining the optimum level for restrictions, termed as 'travel load' herein, to be imposed and evaluates its impact. Furthermore, people globally have faced challenges in adhering to stringent control measures and are less inclined to comply with severe strategies such as social distancing. Although compliance levels with these measures have significantly

decreased, a majority still deems wearing facemasks tolerable if necessary. Therefore, the focus should be on exploring the best compliance levels for vaccination, facemask usage, and travel load. It is noteworthy that enforcing high levels of social distancing, while effective, may not be feasible in an active economy. Thus, in contrast to Najmi et al. (2021), this paper does not underscore social distancing as a core strategy.

In this current study, we delve into the effectiveness of various compliance levels concerning facemask usage, travel load, and vaccination rates, along with their interactions, in suppressing the Delta variant. We employ a disease spread agent-based simulation model specifically developed for Sydney GMA (Najmi et al. 2021a), shedding light on the most efficient combinations of control strategies for pandemics of a similar nature. Furthermore, we conduct a factorial MANOVA analysis to scrutinise the significance of the differences in the impact of diverse compliance levels with the aforementioned control strategies on the attributes of the pandemic.

## Literature review

Since the emergence of the COVID-19 pandemic, several studies have been done all across the globe on the effectiveness of different control strategies such as case isolation (Hellewell et al. 2020), social distancing (Chang et al. 2020; Gomez et al. 2021; Hoertel et al. 2020; Mahdizadeh Gharakhanlou and Hooshangi 2020; Najmi et al. 2021b; Silva et al. 2020a), school closure (Chang et al. 2020; Hoertel et al. 2020; Mahdizadeh Gharakhanlou and Hooshangi 2020; Truszkowska et al. 2021a), vaccination (Livshits et al. 2021; Tata-pudi et al. 2021; Thompson and Wattam 2021), contact tracing (Aleta et al. 2020; Almagor and Picascia 2020; Hinch et al. 2021), and facemask use (Hoertel et al. 2020; Müller et al. 2021; Najmi et al. 2021b; Silva et al. 2020a) to suppress the outbreak of the infection using disease spread agent based models while a lot more researches have been conducted using aggregated mathematical models (Kemp et al. 2021; Kucharski et al. 2020; Vardavas et al. 2020). The results of these studies can serve as a valuable source of information for policymakers and authorities, guiding them in implementing the most effective combination of control strategies to manage pandemics of a similar nature while businesses operate, and the economy remains active.

In the event of a complete lockdown, some research has concentrated on exploring the most efficient control strategies that not only aid authorities in minimising the risk of disease resurgence but also facilitate the reopening of economies by easing stringent restrictions (Livshits et al. 2021). According to the findings of these studies, proper vaccination rate (Panovska-Griffiths et al. 2021; Truszkowska et al. 2021b), facemask use (Najmi et al. 2021b), and implementation of testing and contact tracing (Aleta et al. 2020; Tatapudi et al. 2020) are the suggested strategies to circumvent high compliance of social distancing and reopen economies safely. In another study, the impact of various levels of school reopening on the spread of COVID-19 is examined, utilising a calibrated agent-based model based on data from an urban region in the US (Tatapudi and Das 2021). Their analysis reveals that in the scenario of full school reopening, the total number of infected cases would increase by 8.16%, whereas with a 50% return to school, this growth is smaller, approximately 1.26%. The research suggests a partial return to school, alongside other interventions such as wearing facemasks, practicing social distancing, and maintaining hand hygiene, as effective measures to control the spread of the virus.

All the aforementioned studies utilised attributes such as transmissibility, vaccine effectiveness, incubation, and recovery period, focusing primarily on non-Delta variants of COVID-19. However, the Delta pandemic presents a significant challenge with distinct characteristics. According to a retrospective study by Ong et al. (2021), examining attributes of different variants of SARS-CoV-2, the Delta strain proves to be more contagious and severe, a finding consistent with many other studies (Fisman and Tuite 2021; Mlcochova et al. 2021; Musser et al. 2021; Pasaoglu et al. 2016). Another noteworthy feature contributing to the increased transmissibility of the Delta variant is its shorter incubation period, measuring 4 days, compared to the longer 6-day incubation period for previous variants (Li et al. 2021).

According to an analysis conducted by Musser et al. (2021) vaccination breakthrough cases were about 14% more for Delta infection than all previous variants. Some other research showed a 12–19% reduction in vaccine effectiveness against the B.1.617.2 variant (Delta) compared to their performance against B.1.1.7 (Alpha) after getting the first dose while the difference in efficiency is very small after two doses (Lopez Bernal et al. 2021). Although the efficiency of vaccination against hospitalisation due to the Delta variant was around 90% (Stowe et al. 2021), evidence indicated that vaccination was not influential in slowing down Delta infection spread in India (“Predominance of Delta variant among the COVID-19 vaccinated and unvaccinated individuals, India, May 2021” 2021). These findings imply that although vaccination is effective in preventing severe infections, reducing mortality, and easing the strain on the health system, it may not be equally effective in slowing down the spread of the disease. Vaccinated infectious cases seem to be as contagious as non-vaccinated infectious cases. In this context, based on practical experience, non-pharmaceutical control strategies have proven to be pivotal measures that aided India in navigating through the challenges posed by the Delta pandemic (Yang and Shaman 2021). To examine the Delta pandemic in India, Salvatore et al. (2021) utilised an SIR model to analyse the resurgence of the Delta variant and underscored the significance of early implementation of control strategies. Investigating the precise and comprehensive determination of the optimal and sufficient level of these control strategies is a key criterion.

As of the date of writing this paper, there are only a few research studies within the literature that have focused on the Delta variant of the coronavirus and examined the efficacy of various control strategies in suppressing it, employing a calibrated agent-based model. For instance, in their analysis of various non-pharmaceutical control strategies including school closure, social distancing, and case isolation, Chang et al. (2021) recommended an 80% compliance level with social distancing to bring the Delta pandemic in Sydney under control. While the findings from Chang et al. (2021) caution against reducing the social distancing compliance level, even to 70%, we posit that achieving such a high level of social distancing may prove practically challenging when the economy is open. Additionally, the agent-based parameter calibration in their research is unstructured, and the authors do not account for the interconnected effects between different parameters on pandemic attributes.

In summary, despite numerous studies evaluating the effectiveness of various control strategies in managing non-Delta outbreaks of COVID-19, there is a gap in the literature when it comes to specifically studying the Delta variant using agent-based models and assessing the performance of control strategies. The findings from those studies may not be directly applicable to the Delta pandemic due to distinct disease attributes, such as increased transmissibility and a higher incidence of vaccine breakthrough cases, resulting in lower vaccine effectiveness. This study stands out by exploring the optimal levels of

facemask usage and vaccination rates with minimal risk of disease resurgence while maintaining open activities and a functioning economy. It employs a systematically calibrated agent-based disease spread model developed for Sydney GMA (Najmi et al. 2021a). The insights gained from this study can prove valuable in effectively addressing outbreaks of a similar nature.

## Method

This section is organised as follows: Firstly, Sects. 3–1 provides a detailed explanation of Sydney GMA's transport model and the agent-based disease spread model, serving as the simulation tools employed in this research. Subsequently, Sects. 3–2 outlines the defined target control strategies. Moving on, Sects. 3–3 delves into the metrics utilised for evaluating the effectiveness of various control strategies in pandemic management. Lastly, Sects. 3–4 introduces the statistical approach of MANOVA, which is applied to simulation outputs to investigate the significance of differences in the effects of various compliance levels of control strategies on pandemic attributes.

## Simulation models

To capture patterns of disease transmission throughout the community, this study utilises an agent-based disease spread model introduced by Najmi et al. (2021a). This model has been developed based on the Sydney GMA activity-based model (SydneyGMA model). The authors systematically calibrated the model parameters, encompassing both disease-related and travel behaviour-related aspects, specifically for Sydney GMA. As a result, the model is capable of accurately replicating the number of COVID-19 active cases in Sydney GMA, both on a daily and cumulative basis. Therefore, it serves as an appropriate model for this study, facilitating policy analysis on the impact of various control strategies, as outlined in the evaluation metrics to be defined in Sects. 3–3. The simulation models are detailed in the following.

## Disease transmission model

The disease transmission model used in this analysis is developed based on SydneyGMA by Najmi et al. (2021a) and can simulate the spread of the virus within the population through intra-household relationships and travel for out-of-home activity participation. Agents are assumed to be in one of the seven defined states: infected, vulnerable, exposed, quarantined, quarantined family member, healed, or dead. All agents, except those who are infected, are initially classified as vulnerable. Upon social contact with diseased agents, susceptible agents may probabilistically become infected, transitioning to the exposed state. Exposed agents are in the incubation period, rendering their infections non-contagious. After the incubation period, exposed agents move to the infected category and become contagious. Infected agents, along with their family members, are probabilistically quarantined by authorities and move to quarantined and quarantined family member classes, respectively. Each quarantined family member who becomes infected moves to the quarantined category. After 14 days, the typical period of COVID-19 recovery, infected agents recover and are assumed to be immunised. However, some quarantined agents may die. The unquarantined dead cases are ignored by this simulation. While recovery time may

vary among individuals, and it could be associated with a distribution, we opted for a constant recovery time in our model for the sake of simplicity. It is important to emphasise that this simplification does not compromise the generality of the model. Moreover, unlike (Müller et al. 2021) that explicitly incorporates hospital stays as a distinct state with different time dynamics than home quarantine, we did not differentiate between hospital stays and home quarantine. In this study it is assumed that all infected agents, whether quarantined at home or not, recover (or may die) after 14 days, aligning with the typical recovery period for COVID-19 as reported in the literature (Bhaskar et al. 2020; Eikenberry et al. 2020; Shamil et al. 2021; Tang et al. 2020). A flowchart demonstrating these processes through which an agent's category may change is provided in "Appendix A".

In this paper, the term 'parameter' refers to the estimated weights of variables. The simulation model parameters are classified into three main groups. Firstly, travel behaviour parameters that are associated with SydneyGMA model that influence activity participation rates (and consequently contact rates), activity location, activity start time and duration, and travel modes. These parameters have already been calibrated for Sydney. The second set of parameters is 'policy-related', defining interventions implemented by authorities in response to COVID-19, such as business closures, ultimately leading to changes in trip generation patterns. Policy-related parameters are set according to the target scenarios, and this study's analysis centres on the sensitivity of the disease transmission model to these parameters. The last class of parameters is related to the disease transmission model, specifying virus characteristics and the performance of authorities and the healthcare system. This includes parameters like the incubation period, and probabilities of agents transitioning between states (e.g., exposed to infected, infected to quarantined, infected to healed, quarantined to dead). The parameters in this third class are calibrated to replicate observed data. For a brief summary of the calibration process, please refer to "Appendix B".

## SydneyGMA

SydneyGMA is an agent-based model specifically developed for Sydney GMA, consisting of three primary components: the population synthesiser, network, and demand. The population synthesiser employs an iterative proportional fitting (IPF) method to generate characteristics for households and individuals (e.g., the number of vehicles owned by a household or the gender of individuals) for the 5.8 million residents in Sydney GMA. This IPF method is applied to data collected by the Australian Bureau of Statistics. To determine the travel time for various links in the network, the estimated demand is allocated to different routes within the network component. The computed travel times are subsequently fed back into the demand component, and the updated demand is used to re-estimate the network's travel time. This iterative process continues until the travel times for the network links converge. The demand component in SydneyGMA comprises multiple choice models and a scheduler known as TASHA.

TASHA's prototype was initially introduced by Miller and Roorda (2003), with subsequent enhancements made to incorporate a route-based mode choice model (Miller et al. 2005) and vehicle transactions (Roorda et al. 2009). This Scheduler functions as an agent-based model, generating individual activity schedules through a bottom-up process. Initially, activity episodes are created for individuals, and then activities are organised to form feasible individual schedules. Adjustments, such as shortening or shifting activities, are applied to resolve temporal conflicts. Utilising this information, trip chains are extracted, and potential travel choices, like ridesharing, are simulated based on individuals' sociodemographics, household

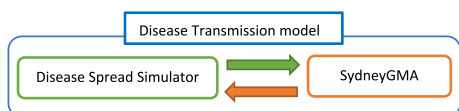
characteristics, and trip patterns within TASHA, using the implemented tour-based mode choice model. While TASHA's primary purpose is the development of travel behaviour and transport policy analysis, it also serves effectively in tracing individuals' contacts and presence in potential transmission places, exposing people to COVID-19. Thus, it provides a mathematical framework for assessing various COVID-19 policies, as explored in this paper.

SydneyGMA strategically allocates public transport trips to specific paths within the transit network, allowing various elements of transit journeys (such as in-vehicle time, walking to/from transit, and waiting and transferring) to be assessed and treated as possible sites for disease transmission. Consequently, the incorporation of SydneyGMA enhances disease spread modelling by factoring in potential locations of transmission. However, it is important to note that SydneyGMA does not specify the particular public transport vehicle used by each agent. Consequently, we choose interacting agents from those employing the public transport mode who share the same destination and activity type, with similar approaching times. Importantly, the assumptions regarding the transport model do not impact the conclusions derived from the relative analysis presented in the [Results](#) section. The primary objective of the paper is not to offer precise forecasts; rather, it aims to evaluate the relative costs and benefits of different confinement policies.

In summary, SydneyGMA simulates the daily activity participation of all residents, capturing details such as the purpose, start and end times, location, and mode of transport, along with the socioeconomic characteristics of each individual. With comprehensive knowledge of individuals' tempo-spatial information, the SydneyGMA model can replicate social contacts, a primary driver of disease spread in communities. SydneyGMA has been employed to construct an agent-based disease transmission model, providing a thorough evaluation of various control strategies. It is important to note a limitation of SydneyGMA: while it simulates activity type, zone, and time on the schedule of each agent, it does not model face-to-face interactions among agents in the same location at a detailed level. Instead, interacting agents are randomly selected from individuals participating in the same activity in the same zone during overlapping times. [Figure 1](#) illustrates the entire simulation process. Given that SydneyGMA replicates individuals' activity participation over a single day, the disease spread simulator frequently runs SydneyGMA to project virus spread over the entire duration of the pandemic, which could span months or years.

Furthermore, in this study, we conducted repeated model runs for each scenario until the virus transmission was eliminated. It's essential to recognize that the number of days varied across scenarios, contingent on the combination of control strategies and the assumed level of compliance in each scenario. This research's simulation scenarios depict hypothetical situations where a typical day is iterated until the virus is eliminated. The trip generation process is managed by TASHA, a strategic model that formulates a typical working day travel schedule for individuals and is utilized to evaluate the impact of policies. However, it lacks the capacity to capture weekly or seasonal patterns, representing a limitation of this research. However, the primary objective of this study is to assess which combination of control strategies had the most substantial impact on pandemic control within these scenarios that could be generated using TASHA.

**Fig. 1** The structure of the disease transmission model





For the analysis in this paper, the travel behaviour parameters and certain disease transmission parameters align with those in Table 1 of Najmi et al. (2021b), representing the calibrated parameters. Meanwhile, disease attributes such as vaccine effectiveness, reproduction rate, facemask efficiency, and infection rate are drawn from existing literature on the Delta variant of COVID-19. Vaccine effectiveness against the Delta variant is reported as 94% for Pfizer and 71% for AstraZeneca after one dose, increasing to 96% and 92%, respectively, after two doses (Stowe et al. 2021). However, alternative studies suggest lower vaccine effectiveness ranging from 79 to 87% for Pfizer against the Delta variant (Lopez Bernal et al. 2021; Nasreen et al. 2021; Sheikh et al. 2021). Considering Pfizer and AstraZeneca as the primary vaccines in Sydney, an average vaccine efficiency of 85% is assumed in this paper's simulation. The reproduction rate ( $R_0$ ) of the Delta variant is higher than ancestral strains, ranging between 3.2 and 8, according to a recent meta-analysis (Liu and Rocklöv 2021). In this paper, the reproduction rate is set to 6, consistent with (Liu et al. 2021). Facemask efficiency is influenced by factors such as mask type (N95, surgical, or cotton), distance between people, etc. (Ueki et al. 2020). A comprehensive review suggests a 67% effectiveness in reducing infection for facemasks against COVID-19 (Chu et al. 2020). While no specific study addresses facemask efficiency with the Delta variant, this paper assumes a 64% efficiency. Concerning the infection rate, the Delta variant's infectiousness is reported as 5 to 9 persons per contact, whereas non-Delta variants have a reduced range of 1.5 to 3.5 (McMorrow 2021). Additionally, parameters related to policy-making and control strategies are configured based on the scenarios to be investigated.

## Control strategies

As previously mentioned, this study focuses on investigating three main control strategies: facemask use, vaccination rate, and travel load. While social distancing (SD) is acknowledged as a key control strategy for disease spread (Najmi et al. 2021b; Silva et al. 2020b), its effectiveness is not explored in this analysis. The intention is to identify the most effective combination of control strategies in a scenario where the economy is open, suggesting a lower level of SD compliance. Nonetheless, it is assumed that a minimum level of SD compliance, set at 50%, is maintained by many people as long as the possibility of infection persists. For simplicity, this study assumes a constant 50% SD compliance across all experiments. The following paragraphs provide a brief explanation of the targeted control strategies in this study.

*Facemask use out of home (FMOH)* To better understand the impact of partial compliance with the facemask control strategy, six different compliance levels are considered in this analysis: 0%, 20%, 40%, 60%, 80%, and 100%. Each compliance level represents the proportion of people in society who wear facemasks outside the home at that particular level. For clarification, a compliance level of 0% signifies that no one uses a facemask, while 100% implies that everyone wears a mask outside the home.

*Vaccination rate (VR)* As discussed in the [introduction](#) section, vaccinating individuals is recognised as an effective control strategy capable of reducing the number of hospitalisations. While the effectiveness of vaccination against the Delta variant is lower compared to previous strains, it remains an essential strategy to confront the outbreak. Similar to the facemask control strategy, this study considers six levels of vaccination rates in society: 0%, 20%, 40%, 60%, 80%, and 100%, where 100% signifies universal vaccination across the entire population.



**Table 1** Control strategies and their implementation in the agent-based transmission model

Control strategy	Implementation approach	Effect on virus spread
Facemask use out of home (FMOH)	Randomly select a population (based on the FMOH rates) representing those who wear a facemask	For the individuals, the infection rate in their contacts is reduced by 67%
Vaccination rate (VR)	Randomly select population (based on the VR rates) representing the vaccinated individuals	For the vaccinated individuals, the infection rate in their contacts is reduced by 90%
Travel load (TL)	Change the trip generation rates based on the TL rates	Fewer trips are generated
Social distancing (SD)	Adjust the contact rates at different activities based on the SD rates	The number of infections in the contacts is reduced

*Travel load (TL)* This variable indicates the extent of an individual's urban mobility within the designated town, which is Sydney GMA in this paper. The term 'travel load' specifically encompasses intra-city trips, with across-the-board trips excluded from the current analysis. The study evaluates five levels of demand load, including 20%, 40%, 60%, 80%, and 100%, to assess their impact on disease spread. To provide context for these levels, 100% implies that people engage in all their activities without any restrictions, similar to the pre-COVID era. Conversely, 20% signifies a scenario in which individuals experience a significant reduction in their freedom to participate in their intended activities, equating to an 80% reduction in activity participation. Recognising the practical impossibility of reducing travel load to zero, the analysis explores a range of possible travel load scenarios, starting from 20%. Table 1 summarises the implementation approach of the aforementioned control strategies in the ABM model.

It is worth mentioning that some studies focused on estimating or reporting actual compliance rates with various control strategies. For instance, Roga et al. (2022) discovered that 62% of their sample exhibited compliance levels exceeding 50%. Examining the first wave of the pandemic, Kleitman et al. (2021) observed compliance rates around 90% in Australia, the UK, USA, and Canada. It is evident that there exists no unanimous consensus on the compliance rate. The current research does not primarily delve into measuring actual compliance rates. It lies in assessing the impact of different compliance rates with various control strategies on pandemic attributes. Hence, we assumed varying levels of compliance and evaluated their effects on pandemic control, akin to the approach taken by Chang et al. (2020) and Mukerjee et al. (2021) among others.

## Evaluation metrics

To assess the effectiveness of different levels of control strategies, it is essential to employ metrics that reflect the pandemic state and attributes during the implementation of these strategies. In this study, four population-level metrics are calculated to gauge the impact of various compliance levels with containment strategies in controlling the pandemic. The reporting period for these metrics spans from the first infection to the last infection in the population, representing the duration until virus elimination. The following sections provide a brief description of these metrics.

*Total infections (TI)* This metric represents the cumulative number of identified infected cases in Sydney GMA from the initial infection to the last infection in the population. Due to the influence of control strategies, individual activities, and transport modes used, daily infections fluctuate throughout the pandemic. TI is calculated by summing the daily infected cases over the entire duration of the pandemic.

*Proportion of reduction (PoR)* This metric serves as a measure corresponding to the reduction in the total number of infections when a specific combination of VR, FMOH, TL, and SD control strategies is implemented, compared to a scenario where no VR and FMOH strategies are in place and TL is at 100%. Essentially, this measure is a restatement of TI and is introduced for a more effective presentation of the population status concerning the spread of infections.

*Virus elimination (VE)* This metric represents the number of days required to eliminate the transmission of the disease within society, reaching a point where individuals no longer face the risk of getting infected by the COVID-19 virus during their out-of-home activities. In this context, the state of zero infections is defined as virus elimination (Dowdle 1998). It is evident that achieving lasting and complete elimination of the virus is nearly impossible,

given the potential for resurgence or the emergence of new variants. In this paper, the term ‘elimination’ is employed in a broader context, intending to convey effective containment within a specific scenario. It is essential to emphasise that the term does not imply a permanent absence but rather signifies a state within the model where virus transmission reaches zero during our simulation process.

*Active case intensity (ACI)* This metric represents the duration, measured in days, during which the number of coexisting infected individuals falls within a specific range. The measure is categorised into three levels: low, medium, and high, denoted as L-ACI, M-ACI, and H-ACI, respectively. The specified intervals correspond to less than 500 active cases for L-ACI, between 500 and 1200 infected individuals for M-ACI, and above 1200 patients for H-ACI. By examining this metric, insights can be gained into the pressure on the healthcare system at each stage, providing valuable information to assess the success of control strategies in managing the pandemic. H-ACI signifies a situation where more than 1200 infected cases coexist simultaneously, leading to high pressure on hospital staff and responsible authorities for care and management.

## Statistical analysis

After conducting experiments for each previously mentioned scenario, the mean of the evaluation metrics is utilised to analyse variance across multiple independent variables using factorial MANOVA. ANOVA (analysis of variance) is a statistical method used to assess the variance of two independent variables on a single dependent variable. Factorial ANOVA extends this basic form to analyse more than two independent variables and a single dependent variable. Factorial MANOVA (multivariate analysis of variance) further extends factorial ANOVA by allowing the use of multiple dependent variables in the analysis.

Factorial MANOVA is an inferential statistical method used to analyse the significance of differences in the impact of various levels of independent variables on multiple dependent variables. In this study, the independent variables are different levels of control strategies, including VR, FMOH, and TL, while evaluation metrics such as TI, PoR, etc., are considered as dependent variables. Factorial MANOVA also provides insights into the magnitude of the effect of the independent variables (control strategies) and their interactions on the dependent variables (evaluation measures). Initially, two statistics, namely Pillai’s Trace and Wilks’ Lambda, are calculated to assess the applicability of MANOVA to our data. The results of these tests are presented in Table 2.

**Table 2** The results of multivariate tests that are conducted to assess the suitability of MANOVA.

Control strategy (independent variable)	Statistics	Value	F	Sig.
FMOH	Pillai’s Trace	3.110	98.428	0.000
	Wilks’ Lambda	0.000	545.985	0.000
VR	Pillai’s Trace	3.401	127.306	0.000
	Wilks’ Lambda	0.000	1033.894	0.000
TL	Pillai’s Trace	2.835	145.271	0.000
	Wilks’ Lambda	0.000	605.894	0.000

As indicated in Table 2, all the statistics are significant, leading to the rejection of the null hypothesis. The null hypothesis posits that all levels of each independent variable have the same effect on dependent variables, and there is no statistically significant difference between those levels. The rejection of the null hypothesis signifies that the differences in the impact of various levels of each independent variable on evaluation metrics (dependent variables) are statistically significant. Therefore, the use of MANOVA is deemed appropriate in this case. To analyse the effect of each control strategy in the absence of others, post-hoc tests are conducted. Additionally, interactive influences of control strategies are plotted to gain a comprehensive perspective on the impact of different combinations of control strategies on pandemic attributes.

## Results

In this section, we will first examine the influence of each control strategy on evaluation metrics individually, utilising MANOVA analysis in Sects. 4.1 Subsequently, in Sects. 4.2 we will explore the interactive effects of these control strategies. Additionally, for interested readers, we present a sensitivity analysis of the calibrated model conducted by Najmi et al. (2021a) in "Appendix B".

### Isolated impact of each control strategy on evaluation metrics

Table 3 consolidates all outputs related to post-hoc tests of MANOVA, aiming to compare the effects of different levels of each control strategy on evaluation metrics in the absence of other control strategies. This information is invaluable for authorities seeking assistance in selecting the best and most efficient containment strategy to limit the outbreak. For each control strategy, two levels, I and J, are defined. The mean of the evaluation metrics for level J is then subtracted from the corresponding mean for level I and inserted into the 'I-J' column in Table 3. For a clearer interpretation of the values in Table 3; Fig. 2 presents a heatmap of the mean difference between two compliance levels (I and J) of control strategies across the evaluation metrics. This figure offers a visual representation of the output obtained from MANOVA post-hoc tests (Table 3). It is crucial to note that some scenarios, such as VR of 100%, are model fictions and improbable to be achieved in reality.

The outputs reveal that both VR and FMOH strategies are positively correlated with PoR, whereas TL has a less strong negative correlation with PoR. The less intense colors in the heatmap of TL also confirm the aforementioned statement. In the case of the Delta outbreak, wearing facemasks during out-of-home activity participation by 80% of individuals can reduce the number of total infections by 31.3%, which is lower than the amount of reduction in non-Delta pandemics (32.7%) obtained by Najmi et al. 's study (2021a).

As Fig. 2 indicates, in the case of a 100% compliance level of FMOH in place, there is a 33.5% reduction in TI, while PoR is 42.1% for the full compliance level of VR. Therefore, VR is a more powerful control strategy than FMOH, assisting in controlling the Delta outbreak by being about 10% more influential in TI reduction. Moreover, 100% adherence to the FMOH strategy has the same impact on PoR as a VR between 40 and 60%, providing further evidence of the substantial role of vaccination in suppressing the Delta outbreak. It is worth mentioning that increasing the level of FMOH results in lower TI until it reaches 80%. After that, increasing the compliance level of FMOH will not lead to a significant reduction in TI.

**Table 3** Results of post-hoc tests of factorial MANOVA

Independent variable	Levels of independent variables		Total infection (TI)		Percent of reduction (PoR)		Virus elimination (VE)					
	Level I (%)	Level J (%)	95% Confidence interval		95% Confidence Interval		95% confidence interval					
			Lower bound	Upper bound	Lower bound	Upper bound	Mean difference (I-J)	Lower bound	Upper bound			
Vaccination Rate	0	20	8.33E+05*	7.84E+05	8.81E+05	8.81E+05	-14.0*	-14.5	-13.4	-27.2*	-35.2	-19.2
		40	1.59E+06*	1.54E+06	1.64E+06	1.64E+06	-26.7*	-27.3	-26.2	-48.3*	-56.3	-40.3
		60	2.21E+06*	2.16E+06	2.26E+06	2.26E+06	-37.1*	-37.7	-36.6	-6.1	-14.1	1.9
		80	2.50E+06*	2.45E+06	2.55E+06	2.55E+06	-42.0*	-42.5	-41.4	112.4*	104.4	120.4
		100	2.51E+06*	2.46E+06	2.56E+06	2.56E+06	-42.1*	-42.7	-41.6	181.4*	173.4	189.4
	20	0	-8.33E+05*	-8.81E+05	-7.84E+05	-7.84E+05	14.0*	13.4	14.5	27.2*	19.2	35.2
		40	7.59E+05*	7.10E+05	8.07E+05	8.07E+05	-12.7*	-13.3	-12.2	-21.1*	-29.1	-13.1
		60	1.38E+06*	1.33E+06	1.43E+06	1.43E+06	-23.2*	-23.7	-22.6	21.1*	13.1	29.1
		80	1.67E+06*	1.62E+06	1.72E+06	1.72E+06	-28.0*	-28.5	-27.5	139.6*	131.6	147.6
		100	1.68E+06*	1.63E+06	1.72E+06	1.72E+06	-28.1*	-28.7	-27.6	208.6*	200.6	216.6
	40	0	-1.59E+06*	-1.64E+06	-1.54E+06	-1.54E+06	26.7*	26.2	27.3	48.3*	40.3	56.3
		20	-7.59E+05*	-8.07E+05	-7.10E+05	-7.10E+05	12.7*	12.2	13.3	21.1*	13.1	29.1
	60	6.20E+05*	5.72E+05	6.69E+05	6.69E+05	-10.4*	-11.0	-9.9	42.2*	34.2	50.2	
	80	9.08E+05*	8.60E+05	9.57E+05	9.57E+05	-15.3*	-15.8	-14.7	160.7*	152.7	168.7	
	100	9.17E+05*	8.69E+05	9.65E+05	9.65E+05	-15.4*	-15.9	-14.9	229.8*	221.8	237.8	

**Table 3** (continued)

Independent variable	Levels of independent variables		Total infection (TI)		Percent of reduction (PoR)		Virus elimination (VE)				
	Level I (%)	Level J (%)	Mean differ-	95% Confidence interval	Mean Differ-	95% Confidence Interval	Mean differ-	95% confidence interval			
			ence (I-J)	Lower bound	Upper bound	ence (I-J)	Lower bound	Upper bound	Lower bound	Upper bound	
60	0	0	- 2.21E+06*	- 2.26E+06	- 2.16E+06	37.1*	36.6	37.7	6.1	- 1.9	14.1
	20	20	- 1.38E+06*	- 1.43E+06	- 1.33E+06	23.2*	22.6	23.7	- 21.1*	- 29.1	- 13.1
	40	40	- 6.20E+05*	- 6.69E+05	- 5.72E+05	10.4*	9.9	11.0	- 42.2*	- 50.2	- 34.2
	80	80	2.88E+05*	2.40E+05	3.36E+05	- 4.8*	- 5.4	- 4.3	118.5*	110.5	126.5
	100	100	2.97E+05*	2.49E+05	3.45E+05	- 5.0*	- 5.5	- 4.4	187.6*	179.6	195.6
80	0	0	- 2.50E+06*	- 2.55E+06	- 2.45E+06	42.0*	41.4	42.5	- 112.4*	- 120.4	- 104.4
	20	20	- 1.67E+06*	- 1.72E+06	- 1.62E+06	28.0*	27.5	28.5	- 139.6*	- 147.6	- 131.6
	40	40	- 9.08E+05*	- 9.57E+05	- 8.60E+05	15.3*	14.7	15.8	- 160.7*	- 168.7	- 152.7
	60	60	- 2.88E+05*	- 3.36E+05	- 2.40E+05	4.8*	4.3	5.4	- 118.5*	- 126.5	- 110.5
	100	100	8.94E+03	- 3.94E+04	5.73E+04	- 0.2	- 0.7	0.4	69.1*	61.1	77.1
100	0	0	- 2.51E+06*	- 2.56E+06	- 2.46E+06	42.1*	41.6	42.7	- 181.4*	- 189.4	- 173.4
	20	20	- 1.68E+06*	- 1.72E+06	- 1.63E+06	28.1*	27.6	28.7	- 208.6*	- 216.6	- 200.6
	40	40	- 9.17E+05*	- 9.65E+05	- 8.69E+05	15.4*	14.9	15.9	- 229.8*	- 237.8	- 221.8
	60	60	- 2.97E+05*	- 3.45E+05	- 2.49E+05	5.0*	4.4	5.5	- 187.6*	- 195.6	- 179.6
	80	80	- 8.94E+03	- 5.73E+04	3.94E+04	0.2	- 0.4	0.7	- 69.1*	- 77.1	- 61.1

**Table 3** (continued)

Independent variable	Levels of independent variables		Total infection (TI)		Percent of reduction (PoR)		Virus elimination (VE)				
	Level I (%)	Level J (%)	95% Confidence interval		Mean Difference (I-J)	95% Confidence Interval		Mean difference (I-J)	95% confidence interval		
			Lower bound	Upper bound		Lower bound	Upper bound		Lower bound	Upper bound	
Proportion of people wearing facemask out of home	0	20	4.16E+05*	3.67E+05	4.64E+05	- 7.0*	- 7.5	- 6.4	- 14.5*	- 22.5	- 6.5
	40	40	8.76E+05*	8.27E+05	9.24E+05	- 14.7*	- 15.3	- 14.2	6.6	- 1.4	14.6
	60	60	1.41E+06*	1.36E+06	1.46E+06	- 23.6*	- 24.2	- 23.1	38.6*	30.6	46.6
	80	80	1.86E+06*	1.82E+06	1.91E+06	- 31.3*	- 31.9	- 30.8	116.2*	108.2	124.2
	100	100	1.99E+06*	1.95E+06	2.04E+06	- 33.5*	- 34.0	- 33.0	198.4*	190.4	206.4
	20	0	- 4.16E+05*	- 4.64E+05	- 3.67E+05	7.0*	6.4	7.5	14.5*	6.5	22.5
	40	40	4.60E+05*	4.12E+05	5.08E+05	- 7.7*	- 8.3	- 7.2	21.2*	13.2	29.2
	60	60	9.91E+05*	9.43E+05	1.04E+06	- 16.6*	- 17.2	- 16.1	53.2*	45.2	61.2
	80	80	1.45E+06*	1.40E+06	1.50E+06	- 24.3*	- 24.9	- 23.8	130.7*	122.7	138.7
	100	100	1.58E+06*	1.53E+06	1.63E+06	- 26.5*	- 27.0	- 26.0	212.9*	204.9	220.9
	40	0	- 8.76E+05*	- 9.24E+05	- 8.27E+05	14.7*	14.2	15.3	- 6.6	- 14.6	1.4
	20	20	- 4.60E+05*	- 5.08E+05	- 4.12E+05	7.7*	7.2	8.3	- 21.2*	- 29.2	- 13.2
	60	60	5.32E+05*	4.83E+05	5.80E+05	- 8.9*	- 9.5	- 8.4	32.0*	24.0	40.0
	80	80	9.89E+05*	9.41E+05	1.04E+06	- 16.6*	- 17.1	- 16.1	109.6*	101.6	117.6
	100	100	1.12E+06*	1.07E+06	1.17E+06	- 18.8*	- 19.3	- 18.2	191.8*	183.8	199.8
	60	0	- 1.41E+06*	- 1.46E+06	- 1.36E+06	23.6*	23.1	24.2	- 38.6*	- 46.6	- 30.6
20	20	- 9.91E+05*	- 1.04E+06	- 9.43E+05	16.6*	16.1	17.2	- 53.2*	- 61.2	- 45.2	
40	40	- 5.32E+05*	- 5.80E+05	- 4.83E+05	8.9*	8.4	9.5	- 32.0*	- 40.0	- 24.0	
80	80	4.57E+05*	4.09E+05	5.06E+05	- 7.7*	- 8.2	- 7.1	77.6*	69.6	85.6	
100	100	5.87E+05*	5.38E+05	6.35E+05	- 9.9*	- 10.4	- 9.3	159.8*	151.8	167.8	



**Table 3** (continued)

Independent variable	Levels of independent variables		Total infection (TI)		Percent of reduction (PoR)		Virus elimination (VE)				
	Level I (%)	Level J (%)	Mean difference (I-J)	95% Confidence interval	Mean Difference (I-J)	95% Confidence Interval	Mean difference (I-J)	95% confidence interval			
									Lower bound	Upper bound	Lower bound
80	0	0	-1.86E+06*	-1.91E+06	-1.82E+06	31.3*	30.8	31.9	-116.2*	-124.2	-108.2
	20	20	-1.45E+06*	-1.50E+06	-1.40E+06	24.3*	23.8	24.9	-130.7*	-138.7	-122.7
	40	40	-9.89E+05*	-1.04E+06	-9.41E+05	16.6*	16.1	17.1	-109.6*	-117.6	-101.6
	60	60	-4.57E+05*	-5.06E+05	-4.09E+05	7.7*	7.1	8.2	-77.6*	-85.6	-69.6
	100	100	1.29E+05*	8.09E+04	1.78E+05	-2.2*	-2.7	-1.6	82.2*	74.2	90.2
100	0	0	-1.99E+06*	-2.04E+06	-1.95E+06	33.5*	33.0	34.0	-198.4*	-206.4	-190.4
	20	20	-1.58E+06*	-1.63E+06	-1.53E+06	26.5*	26.0	27.0	-212.9*	-220.9	-204.9
	40	40	-1.12E+06*	-1.17E+06	-1.07E+06	18.8*	18.2	19.3	-191.8*	-199.8	-183.8
	60	60	-5.87E+05*	-6.35E+05	-5.38E+05	9.9*	9.3	10.4	-159.8*	-167.8	-151.8
	80	80	-1.29E+05*	-1.78E+05	-8.09E+04	2.2*	1.6	2.7	-82.2*	-90.2	-74.2

**Table 3** (continued)

Independent variable	Levels of independent variables		Total infection (TI)		Percent of reduction (PoR)		Virus elimination (VE)				
	Level I (%)	Level J (%)	95% Confidence interval		Mean Differ-ence (I-J)	95% Confidence Interval		Mean differ-ence (I-J)	95% confidence interval		
			Lower bound	Upper bound		Lower bound	Upper bound		Lower bound	Upper bound	
Demand Load	20	40	- 4.80E+05*	- 5.22E+05	- 4.38E+05	8.1*	7.6	8.5	- 109.6*	- 116.6	- 102.6
		60	- 9.46E+05*	- 9.89E+05	- 9.04E+05	15.9*	15.4	16.4	- 121.5*	- 128.5	- 114.5
		80	- 1.30E+06*	- 1.34E+06	- 1.25E+06	21.8*	21.3	22.3	- 149.2*	- 156.2	- 142.2
		100	- 1.58E+06*	- 1.62E+06	- 1.54E+06	26.5*	26.1	27.0	- 150.1*	- 157.1	- 143.1
		40	4.80E+05*	4.38E+05	5.22E+05	- 8.1*	- 8.5	- 7.6	109.6*	102.6	116.6
		60	- 4.66E+05*	- 5.09E+05	- 4.24E+05	7.8*	7.4	8.3	- 11.9*	- 18.9	- 4.9
		80	- 8.17E+05*	- 8.59E+05	- 7.75E+05	13.7*	13.2	14.2	- 39.6*	- 46.6	- 32.6
		100	- 1.10E+06*	- 1.14E+06	- 1.06E+06	18.5*	18.0	18.9	- 40.5*	- 47.5	- 33.5
		20	9.46E+05*	9.04E+05	9.89E+05	- 15.9*	- 16.4	- 15.4	121.5*	114.5	128.5
		40	4.66E+05*	4.24E+05	5.09E+05	- 7.8*	- 8.3	- 7.4	11.9*	4.9	18.9
		80	- 3.51E+05*	- 3.93E+05	- 3.08E+05	5.9*	5.4	6.4	- 27.7*	- 34.7	- 20.7
		100	- 6.34E+05*	- 6.76E+05	- 5.91E+05	10.6*	10.2	11.1	- 28.6*	- 35.6	- 21.6
	20	1.30E+06*	1.25E+06	1.34E+06	- 21.8*	- 22.3	- 21.3	149.2*	142.2	156.2	
	40	8.17E+05*	7.75E+05	8.59E+05	- 13.7*	- 14.2	- 13.2	39.6*	32.6	46.6	
	60	3.51E+05*	3.08E+05	3.93E+05	- 5.9*	- 6.4	- 5.4	27.7*	20.7	34.7	
	100	- 2.83E+05*	- 3.25E+05	- 2.41E+05	4.8*	4.3	5.2	- 0.9	- 7.9	6.1	
	20	1.58E+06*	1.54E+06	1.62E+06	- 26.5*	- 27.0	- 26.1	150.1*	143.1	157.1	
	40	1.10E+06*	1.06E+06	1.14E+06	- 18.5*	- 18.9	- 18.0	40.5*	33.5	47.5	
	60	6.34E+05*	5.91E+05	6.76E+05	- 10.6*	- 11.1	- 10.2	28.6*	21.6	35.6	
	80	2.83E+05*	2.41E+05	3.25E+05	- 4.8*	- 5.2	- 4.3	0.9	- 6.1	7.9	

**Table 3** (continued)

Independent variable	Levels of independent variables	Number of active cases less than 500 (L-ACI)		Number of active cases between 500 and 12,000 (M-ACI)		Number of active cases above 12,000 (H-ACI)					
		Mean difference (I-J)	95% Confidence interval		Mean difference (I-J)	95% Confidence interval		Mean difference (I-J)	95% Confidence interval		
			Lower bound	Upper bound		Lower bound	Upper bound		Lower bound	Upper bound	
Vaccination Rate	0	20	-8.2*	-12.0	-4.4	-25.2*	-29.7	-20.8	7.9*	5.6	10.3
	40	40	-27.0*	-30.8	-23.1	-37.9*	-42.3	-33.4	18.6*	16.3	21.0
	60	60	-44.8*	-48.6	-40.9	0.1	-4.3	4.6	38.9*	36.5	41.2
	80	80	5.0*	1.1	8.8	32.0*	27.5	36.4	75.3*	73.0	77.7
	100	100	42.8*	39.0	46.7	62.1*	57.7	66.6	75.3*	73.0	77.7
	20	0	8.2*	4.4	12.0	25.2*	20.8	29.7	-7.9*	-10.3	-5.6
	40	40	-18.8*	-22.6	-14.9	-12.6*	-17.1	-8.2	10.7*	8.4	13.0
	60	60	-36.6*	-40.4	-32.7	25.4*	20.9	29.8	30.9*	28.6	33.3
	80	80	13.2*	9.3	17.0	57.2*	52.7	61.7	67.4*	65.1	69.7
	100	100	51.0*	47.2	54.9	87.4*	82.9	91.8	67.4*	65.1	69.7
40	0	27.0*	23.1	30.8	37.9*	33.4	42.3	-18.6*	-21.0	-16.3	
60	20	18.8*	14.9	22.6	12.6*	8.2	17.1	-10.7*	-13.0	-8.4	
80	60	-17.8*	-21.6	-14.0	38.0*	33.5	42.5	20.2*	17.9	22.6	
100	80	31.9*	28.1	35.8	69.8*	65.4	74.3	56.7*	54.4	59.0	
100	100	69.8*	66.0	73.6	100.0*	95.5	104.5	56.7*	54.4	59.0	

**Table 3** (continued)

Independent variable	Levels of independent variables	Number of active cases less than 500 (L-ACI)		Number of active cases between 500 and 12,000 (M-ACI)		Number of active cases above 12,000 (H-ACI)				
		Mean difference (L-I)	95% Confidence interval		Mean difference (I-I)	95% Confidence interval		Mean difference (I-I)	95% Confidence interval	
			Lower bound	Upper bound		Lower bound	Upper bound		Lower bound	Upper bound
60	0	44.8*	40.9	48.6	-0.1	-4.6	4.3	-38.9*	-41.2	-36.5
	20	36.6*	32.7	40.4	-25.4*	-29.8	-20.9	-30.9*	-33.3	-28.6
	40	17.8*	14.0	21.6	-38.0*	-42.5	-33.5	-20.2*	-22.6	-17.9
	80	49.7*	45.9	53.6	31.8*	27.4	36.3	36.5*	34.1	38.8
	100	87.6*	83.8	91.4	62.0*	57.5	66.5	36.5*	34.1	38.8
80	0	-5.0*	-8.8	-1.1	-32.0*	-36.4	-27.5	-75.3*	-77.7	-73.0
	20	-13.2*	-17.0	-9.3	-57.2*	-61.7	-52.7	-67.4*	-69.7	-65.1
	40	-31.9*	-35.8	-28.1	-69.8*	-74.3	-65.4	-56.7*	-59.0	-54.4
	60	-49.7*	-53.6	-45.9	-31.8*	-36.3	-27.4	-36.5*	-38.8	-34.1
	100	37.9*	34.0	41.7	30.2*	25.7	34.6	0.0	-2.3	2.3
100	0	-42.8*	-46.7	-39.0	-62.1*	-66.6	-57.7	-75.3*	-77.7	-73.0
	20	-51.0*	-54.9	-47.2	-87.4*	-91.8	-82.9	-67.4*	-69.7	-65.1
	40	-69.8*	-73.6	-66.0	-100.0*	-104.5	-95.5	-56.7*	-59.0	-54.4
	60	-87.6*	-91.4	-83.8	-62.0*	-66.5	-57.5	-36.5*	-38.8	-34.1
	80	-37.9*	-41.7	-34.0	-30.2*	-34.6	-25.7	0.0	-2.3	2.3

**Table 3** (continued)

Independent variable	Levels of independent variables	Number of active cases less than 500 (L-ACI)		Number of active cases between 500 and 12,000 (M-ACI)		Number of active cases above 12,000 (H-ACI)					
		Mean difference (I-J)	95% Confidence interval Lower bound Upper bound	Mean difference (I-J)	95% Confidence interval Lower bound Upper bound	Mean difference (I-J)	95% Confidence interval Lower bound Upper bound				
	Level I (%)	Level J (%)									
Proportion of people wearing facemask out of home	0	20	- 17.0*	- 20.8	- 13.2	- 10.4*	- 14.9	- 6.0	12.4*	10.0	14.7
		40	- 3.6	- 7.4	0.3	- 4.7*	- 9.2	- 0.2	12.7*	10.4	15.1
		60	17.0*	13.2	20.9	- 8.5*	- 13.0	- 4.1	28.2*	25.9	30.5
		80	28.6*	24.7	32.4	39.3*	34.9	43.8	45.6*	43.3	48.0
		100	58.0*	54.2	61.9	70.3*	65.8	74.7	67.0*	64.6	69.3
	20	0	17.0*	13.2	20.8	10.4*	6.0	14.9	- 12.4*	- 14.7	- 10.0
		40	13.4*	9.6	17.3	5.7*	1.3	10.2	0.4	- 2.0	2.7
		60	34.0*	30.2	37.9	1.9	- 2.6	6.4	15.8*	13.5	18.2
		80	45.6*	41.7	49.4	49.8*	45.3	54.2	33.3*	30.9	35.6
		100	75.0*	71.2	78.9	80.7*	76.2	85.2	54.6*	52.3	56.9

Independent variable	Levels of independent variables	Number of active cases less than 500 (L-ACI)				Number of active cases between 500 and 12,000 (M-ACI)				Number of active cases above 12,000 (H-ACI)			
		Mean difference (L-I)		95% Confidence interval		Mean difference (L-I)		95% Confidence interval		Mean difference (L-I)		95% Confidence interval	
		Level I (%)	Level J (%)	Lower bound	Upper bound	Lower bound	Upper bound	Lower bound	Upper bound	Lower bound	Upper bound	Lower bound	Upper bound
Table 3 (continued)	40	0	3.6	-0.3	7.4	4.7*	0.2	9.2	-12.7*	-15.1	-10.4		
		20	-13.4*	-17.3	-9.6	-5.7*	-10.2	-1.3	-0.4	-2.7	2.0		
		60	20.6*	16.8	24.4	-3.8	-8.3	0.6	15.5*	13.1	17.8		
		80	32.1*	28.3	36.0	44.0*	39.6	48.5	32.9*	30.6	35.2		
		100	61.6*	57.8	65.4	75.0*	70.5	79.4	54.2*	51.9	56.6		
	60	0	-17.0*	-20.9	-13.2	8.5*	4.1	13.0	-28.2*	-30.5	-25.9		
		20	-34.0*	-37.9	-30.2	-1.9	-6.4	2.6	-15.8*	-18.2	-13.5		
		40	-20.6*	-24.4	-16.8	3.8	-0.6	8.3	-15.5*	-17.8	-13.1		
		80	11.5*	7.7	15.4	47.9*	43.4	52.3	17.4*	15.1	19.8		
		100	41.0*	37.2	44.8	78.8*	74.3	83.3	38.8*	36.4	41.1		
80	0	-28.6*	-32.4	-24.7	-39.3*	-43.8	-34.9	-45.6*	-48.0	-43.3			
	20	-45.6*	-49.4	-41.7	-49.8*	-54.2	-45.3	-33.3*	-35.6	-30.9			
	40	-32.1*	-36.0	-28.3	-44.0*	-48.5	-39.6	-32.9*	-35.2	-30.6			
	60	-11.5*	-15.4	-7.7	-47.9*	-52.3	-43.4	-17.4*	-19.8	-15.1			
	100	29.5*	25.6	33.3	30.9*	26.5	35.4	21.3*	19.0	23.7			
100	0	-58.0*	-61.9	-54.2	-70.3*	-74.7	-65.8	-67.0*	-69.3	-64.6			
	20	-75.0*	-78.9	-71.2	-80.7*	-85.2	-76.2	-54.6*	-56.9	-52.3			
	40	-61.6*	-65.4	-57.8	-75.0*	-79.4	-70.5	-54.2*	-56.6	-51.9			
	60	-41.0*	-44.8	-37.2	-78.8*	-83.3	-74.3	-38.8*	-41.1	-36.4			
	80	-29.5*	-33.3	-25.6	-30.9*	-35.4	-26.5	-21.3*	-23.7	-19.0			

**Table 3** (continued)

Independent variable	Levels of independent variables		Number of active cases less than 500 (L-ACI)		Number of active cases between 500 and 12,000 (M-ACI)		Number of active cases above 12,000 (H-ACI)				
	Level I (%)	Level J (%)	95% Confidence interval		95% Confidence interval		95% Confidence interval				
			Lower bound	Upper bound	Lower bound	Upper bound	Lower bound	Upper bound			
Demand Load	20	40	-27.1*	-30.5	-23.8	-61.1*	-65.0	-57.2	-20.3*	-22.4	-18.3
		60	-22.7*	-26.0	-19.3	-56.2*	-60.1	-52.3	-43.3*	-45.4	-41.3
		80	-49.6*	-53.0	-46.3	-55.4*	-59.3	-51.5	-44.9*	-47.0	-42.9
		100	-39.3*	-42.7	-36.0	-58.7*	-62.6	-54.8	-52.7*	-54.8	-50.7
	40	20	27.1*	23.8	30.5	61.1*	57.2	65.0	20.3*	18.3	22.4
		60	4.4*	1.1	7.8	4.9*	1.0	8.8	-23.0*	-25.0	-21.0
		80	-22.5*	-25.8	-19.1	5.7*	1.8	9.6	-24.6*	-26.6	-22.5
		100	-12.2*	-15.5	-8.8	2.4	-1.5	6.3	-32.4*	-34.4	-30.3
	60	20	22.7*	19.3	26.0	56.2*	52.3	60.1	43.3*	41.3	45.4
		40	-4.4*	-7.8	-1.1	-4.9*	-8.8	-1.0	23.0*	21.0	25.0
	80	-26.9*	-30.3	-23.6	0.8	-3.1	4.7	-1.6	-3.6	0.5	
	100	-16.6*	-20.0	-13.3	-2.5	-6.4	1.4	-9.4*	-11.4	-7.3	
80	20	49.6*	46.3	53.0	55.4*	51.5	59.3	44.9*	42.9	47.0	
	40	22.5*	19.1	25.8	-5.7*	-9.6	-1.8	24.6*	22.5	26.6	
	60	26.9*	23.6	30.3	-0.8	-4.7	3.1	1.6	-0.5	3.6	
	100	10.3*	6.9	13.6	-3.3	-7.2	0.6	-7.8*	-9.8	-5.8	
100	20	39.3*	36.0	42.7	58.7*	54.8	62.6	52.7*	50.7	54.8	
	40	12.2*	8.8	15.5	-2.4	-6.3	1.5	32.4*	30.3	34.4	
	60	16.6*	13.3	20.0	2.5	-1.4	6.4	9.4*	7.3	11.4	
	80	-10.3*	-13.6	-6.9	3.3	-0.6	7.2	7.8*	5.8	9.8	



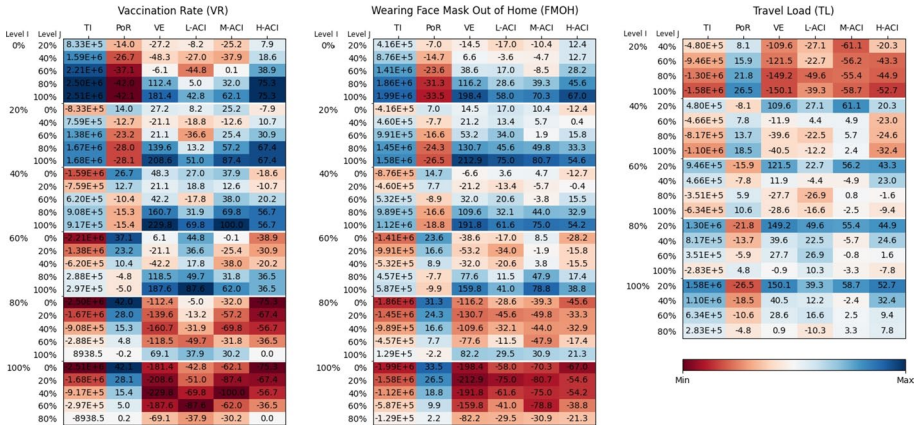
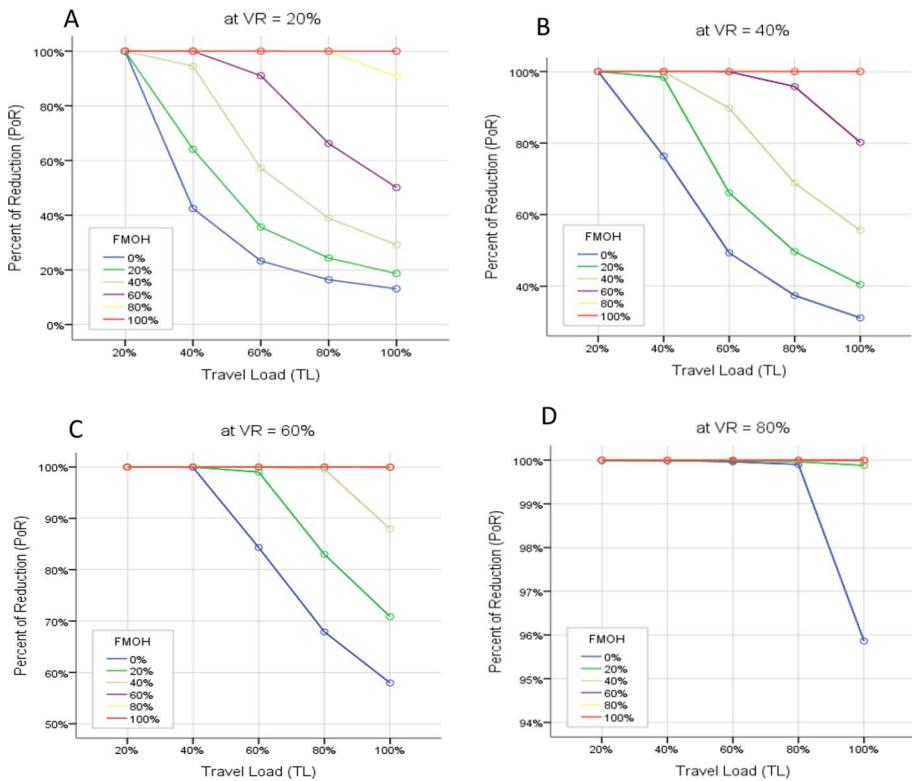


Fig. 2 The heatmap of the difference (I-J) between the means of the evaluation metrics (TI, PoR, VE, L-ACI, M-ACI, H-ACI) for two different levels of control strategies (level I and level J), calculated by Factorial MANOVA

Another control strategy included in this analysis is TL, which is negatively correlated with TI. In other words, a lower level of TL will lead to a higher PoR. In the case of normal traffic load (100%), where everyone participates in their desired out-of-home activities, PoR is 18.4% less than a situation where TL is reduced to 20%. Although reducing TL can be a useful strategy to decrease TI, it is not as powerful as VR or FMOH, as an 80% TL reduction has the same influence as a 40% increase in VR and around a 60% increase in FMOH. Due to this fact, it may be possible to keep the economy open at a 50% compliance level of social distancing while appropriate levels of FMOH and VR are in place during the pandemic.

In the case of achieving a vaccination rate of 80% and 100%, the total number of days required to control the Delta pandemic is 112 and 181 days less than the situation where no one gets vaccinated, representing a significant reduction in time. For vaccination rates of 20% and 40%, the Vaccine Efficacy (VE) increases by 27 and 48 days, respectively, due to the interruption in herd immunisation, while VE is not statistically significant for a vaccination rate of 60%. An FMOH compliance level of 20%, similar to VRs of 20% and 40%, causes a delay in herd immunisation, resulting in 14.5 more days needed to eliminate the virus. However, increasing the compliance level from 40 to 100% shortens the number of days required to control the Delta pandemic. For instance, when 80% of individuals are wearing facemasks outside their homes, virus elimination occurs 116 days earlier than in the case of not having an FMOH control strategy in place.

As expected, an increase in TL can result in a longer period needed to eliminate the virus. For instance, in the case of 100% TL, it takes 150 days more to defeat the virus and remove it from society compared to TL of 20%. Although reducing TL seems to be an influential control strategy to shorten VE, sticking to the other two control strategies, VR and FMOH, would be more beneficial in terms of eliminating infections while reopening businesses. In this regard, a VR between 80 and 100% is as influential as reducing TL from 100 to 20%. Additionally, an 80-100% compliance level of FMOH can also benefit society in terms of reducing pandemic life, similar to decreasing TL to 20%. This would guarantee a more powerful effect of a combination of FMOH and VR in place compared to applying restrictions to businesses to implement lower TL.



**Fig. 3** Interactive influence of FMOH and TL on the percent reduction of the total number of infected cases (PoR) at VR = 20% (a), VR = 40% (b), VR = 60% (c), and VR = 80% (d)

In the case of H-ACI, indicating a high level of stress on the healthcare system, VR appears to be the most effective control strategy. Achieving 80% VR can reduce the number of days with more than 1200 infections by 75 days. In terms of H-ACI, there is no significant difference between 80% and 100% VR. FMOH also proves to be an effective control strategy to alleviate pressure on the health system, as 100% FMOH can reduce the number of days with High Active Case Intensity by 70 days. The impact of TL's reduction to 20% on shortening the H-ACI period is not as significant as VR and FMOH, and it can reduce it at most by 52 days. According to Fig. 2, considering M-ACI and L-ACI, boosting the compliance level of FMOH and VR will initially cause an interruption in herd immunisation, but by reaching 80%, it will immunise the society and therefore shorten the number of days in which 500 to 1200 infections occurred, leading to the alleviation of pressure on the health protection system.

\*The mean difference is significant at the 0.05 level.

### Interactive impact of control strategies on evaluation metrics

Figure 3, 4 and 5 provide illustrations of the interaction between defined control strategies and their impact on evaluating measures by plotting computed marginal means for runs. Figure 3 shows the interactive effect of FMOH and TL on the percent reduction of total

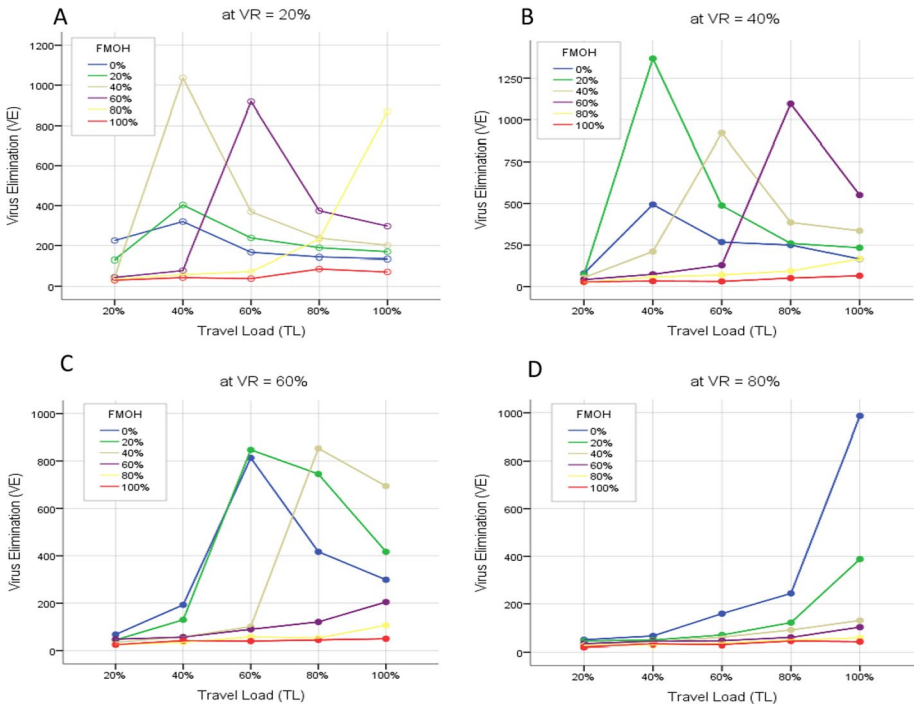


**Fig. 4** Interactive influence of FMOH and TL on the number of days it takes to eliminate the virus (VE) at VR = 20% (a), VR = 40% (b), VR = 60% (c), and VR = 80% (d)

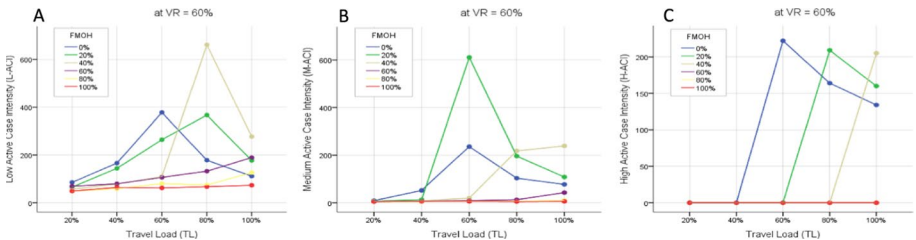


**Fig. 5** Interactive influence of FMOH and TL control strategies on the number of days during which the number of active cases (ACI) is low (L-ACI) (A), moderate (M-ACI) (B), and high (H-ACI) (C) at a vaccination rate of 60%

infections at several vaccination rates such as 20%, 40%, 60%, and 80%. The figures for 0% and 100% VR are not included here as (1) we assume all countries started vaccinating people and (2) 100% VR may be unattainable in practice. A reducing sensitivity of PoR to TL and FMOH can be observed across Fig. 3a, d. As Fig. 3a indicates, at lower vaccination rates, PoR shows the most sensitivity to the FMOH compliance level and travel load. The higher the travel load, the lower the PoR, and a rise in FMOH compliance level would lead to a higher reduction in total infections and therefore higher PoR. In contrast, where VR grows and reaches 80%, as shown in Fig. 3d, PoR is not reliant on FMOH and TL unless at 100%

TL and zero compliance with FMOH. According to Fig. 3d, maintaining a minimum of 20% compliance level of FMOH together with 80% VR is a practical approach that will lead to pandemic control while TL is as pre-COVID (100%). In case the enforcement of 20% FMOH is not desirable, a reduction of travel load to 80% should be in place to obtain the same result.

As shown in Fig. 3c, wearing facemasks by less than 40% of people while the VR is 60% would not be an efficient strategy at 100% TL, even though it will result in a 58–88% reduction in overall infections based on the FMOH level abided by individuals. At 60% VR, the minimum safe level of FMOH strategy compliance appears to be 60%. As a result, 60% VR with 60% FMOH is a viable alternative to 80% VR and 20% FMOH for controlling the Delta epidemic while restoring the economy. This implies that VR and FMOH are complementary control strategies so that a lack of compliance with one can be offset by a higher level of compliance with the other.

The interactive effect of control measures on the number of days it takes to eliminate the virus (VE) is depicted in Fig. 4. As indicated in Fig. 4a, at 20% VR and 40% or more TL, virus elimination happens earlier at low and high levels of FMOH than at the medium levels. At low levels of FMOH, herd immunisation and virus elimination occur naturally and earlier but at the cost of a high number of infections, as can be seen in Fig. 3a. Whereas, at high levels of FMOH, the society would be immunised as a result of the FMOH control strategy, which results in virus elimination in fewer days and a low number of illnesses. FMOH interrupts herd immunisation at intermediate compliance levels, resulting in a longer time to eliminate the virus than in previous cases but with fewer infections compared to lower FMOH compliance levels.

A similar explanation applies to the relationship between VE and TL at a constant level of FMOH. At lower vaccination rates, the relationship between VE and TL is also not uniform. Considering a constant compliance level of FMOH, such as 40%, is in place at 40% VR, for example, as seen in Fig. 4b, VE is shorter at low and high travel loads, while it takes a longer time for the virus to be eliminated at intermediate travel loads. This occurs as a result of the interruption of TL in the formation of herd immunisation. When TL falls significantly, however, it leads to herd immunity and a shorter VE with fewer infected cases. When TL is 100%, herd immunisation occurs naturally in a shorter amount of time, though at the cost of a greater number of infections.

Furthermore, because the vaccine can cause herd immunisation, both the relationship between VE and FMOH and the relationship between VE and TL begin to act monotonously as VR grows, and moderate compliance levels with FMOH and TL will no longer cause an interruption in herd immunisation. The VE trends, for example, are largely monotonous and ascending at a VR of 80%, as seen in Fig. 4d. The lower the TL and the higher the FMOH compliance, the sooner the infection will be destroyed. However, with an FMOH level of 80% or above, virus elimination is independent of the travel load and is at its minimum amount, which is around 50 days. In terms of virus elimination, there is a considerable difference between the 80% and 100% travel load at zero FMOH while VR is 80%. At 100% TL, a small increase in FMOH to 20% would result in a 600-day reduction in VE.

At a VR of 60%, Fig. 5 depicts the interactive effect of TL and FMOH on each category of active case intensity (L-ACI, M-ACI, and H-ACI). The number of days the society experiences L-ACI is much smaller at low and high levels of FMOH and TL than at medium levels of them, where L-ACI is longer due to the deleterious influence of the aforementioned control strategies on natural herd immunisation (Fig. 5A). It's also worth noting that the L-ACI pattern is different for FMOH levels of 60% or above, and it rises as TL rises.

The role of control strategies in relieving pressure on the healthcare system can be investigated using Figs. 4c and 5b. Under 60% of VR and a 60% compliance level of FMOH,

even if there are no limitations on travel load, high and medium ACI (H-ACI, M-ACI) are approximately zero, implying no strain on the health sector. In other words, the number of days when the number of coexisting infected cases is between 500 and 12,000 or over 12,000 is near zero, and therefore, the healthcare system only experiences days with no more than 500 patients, which is easier to manage with less stress.

## Conclusion

Utilising an agent-based disease spread model based on SydneyGMA, an activity-based transport model developed for the Sydney Greater Metropolitan Area, this study investigates the interactive effects of various combinations of control strategies, such as vaccination rate (VR), face mask use out of home (FMOH), and travel load (TL), on managing the Delta outbreak in Sydney GMA. Several measures, including total infection (TI), proportion of reduction (PoR), virus elimination (VE), and active case intensity (ACI), are defined to quantitatively characterise pandemic situations and facilitate a precise evaluation of the impact of control strategies on the pandemic. To specifically analyze the outbreak caused by the Delta variant of COVID-19, disease attributes were extracted from existing literature on Delta and incorporated into the model. Using agent-based models for pandemic studies offers advantages over other methods, such as aggregate ones. Despite requiring more data, the activity-based model embedded in agent-based models captures the dynamics of individuals' interactions while traveling across the city to engage in their activities, allowing for a more detailed and reliable analysis of virus spread in potential transmission places within the community. This approach provides valuable insights for policymaking regarding pandemic control.

The simulation results indicate that wearing facemasks during outdoor activities can lead to a 33.5% reduction in the total number of infections caused by the Delta virus. This percentage increases to 42.1% when everyone is vaccinated. As highlighted in the results section, full compliance with the FMOH strategy yields an equivalent impact on total infection reduction as a vaccination rate ranging from 40 to 60%. Consequently, the findings of this research position vaccination rate as a more potent control strategy compared to facemask usage for addressing the Delta pandemic. Among the three factors considered—facemask usage, vaccination rate, and travel load—reducing travel load emerges as the least effective control strategy. This is evidenced by the fact that decreasing travel load from 100 to 20% has a comparable impact on lowering the overall number of infections as increasing the vaccination rate by 40%.

suppressing the spread of the Delta variant proved to be more challenging than previous strains, as evidenced by the reduced efficacy of containment strategies (as observed in the comparison with Najmi et al. (2021b)). Our study emphasises the positive impact of implementing a combination of 60% vaccination rate (VR) and a 60% compliance level with the FMOH strategy in controlling the Delta spread in Sydney, with the travel load (TL) remaining as it was pre-COVID. This suggests the potential for keeping businesses open and lifting restrictions. Even with an 80% or higher vaccination rate, pandemic control is achievable with 20% compliance level with the FMOH strategy. Another equally effective alternative entails a 40% vaccination rate paired with an 80% compliance level with the FMOH strategy. Providing quantitative insights into the effectiveness of common control strategies in suppressing the Delta strain outbreak of COVID-19, this study aims to inform policymakers about the potential outcomes of their pandemic control decisions. It aids in devising efficient regulations that balance disease control with individual satisfaction and convenience. The

proposed control measures not only empower authorities to implement successful pandemic control policies for Delta outbreak or future pandemics of similar nature but also contribute to societal satisfaction by suggesting the relaxation of travel load limitations. This, in turn, allows people to engage in their desired activities as they did pre-pandemic, contingent upon adhering to the specified levels of VR, FMOH, and social distancing.

Finally, it is important to note that the results may not be directly applicable to urban areas other than Sydney GMA. While the policy-related parameters and parameters of the disease spread agent-based model might be consistent across various areas, the travel behaviour-related parameters, which capture activity participation and trips of individuals, are area-specific and need to be calibrated for the desired region.

**Open Access** This article is licensed under a Creative Commons Attribution 4.0 International License, which permits use, sharing, adaptation, distribution and reproduction in any medium or format, as long as you give appropriate credit to the original author(s) and the source, provide a link to the Creative Commons licence, and indicate if changes were made. The images or other third party material in this article are included in the article's Creative Commons licence, unless indicated otherwise in a credit line to the material. If material is not included in the article's Creative Commons licence and your intended use is not permitted by statutory regulation or exceeds the permitted use, you will need to obtain permission directly from the copyright holder. To view a copy of this licence, visit <http://creativecommons.org/licenses/by/4.0/>.

## Appendix A

The following Fig. 6 illustrates the process through which an agent's category may change within the disease spread simulator.

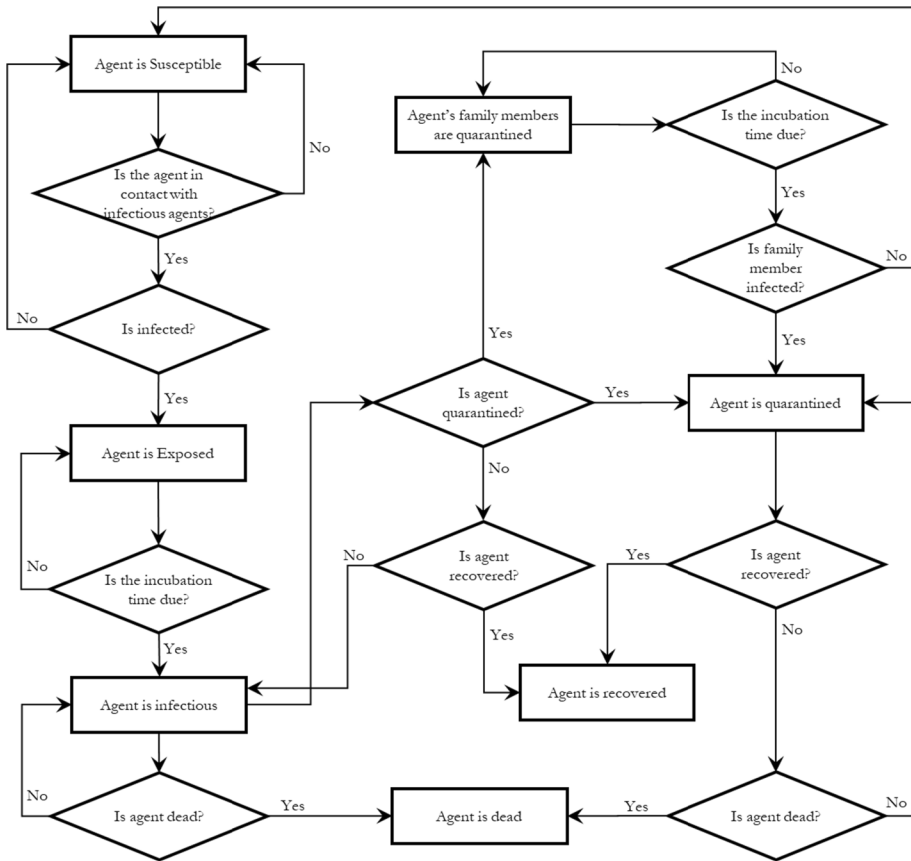


Fig. 6 The disease spread simulator flowchart (Najmi et al. 2021a)

## Appendix B

Different agent-based models are utilised in the literature to estimate the progression of COVID-19 spread and evaluate strategies to control the outbreak of the infectious disease. However, disease spread estimations in the literature are often based on observational epidemiologic studies, essentially aggregated models that may not be directly applicable to agent-based models. Consequently, these models need calibration. The parameters influencing disease spread are highly interrelated, and their effects on simulation outputs should be considered. Recognising these interactions, a set of parameters must be calibrated simultaneously to capture their combined effects. To address this, Najmi et al. (2021a) implemented a response surface methodology (RSM)-based approach to calibrate parameters for SydneyGMA, taking into account their mutual effects. RSM involves a set of mathematical and statistical techniques used to develop, improve, and optimise processes where a response of interest is influenced by several factors, with the ultimate goal of optimising the response.



The calibrated parameters included infection probability per contact, infection probability at home, quarantine probability, base contact number, contact number in transit, and incubation period. A feasible range for each calibration parameter (as input to the RSM) was specified, indicating the range within which the optimal value would likely fall. For instance, the incubation period had a feasible range of 3 to 6 days, with values closer to 4.5 having a higher probability of selection based on previous research (Guan et al. 2020). The contact number had a feasible range set between 1 to 3 contacts. The base contact number was assumed to be occupation-dependent, higher for community service workers and sales workers by a factor of 1 to 1.5. The base contact number in transit was considered higher, within the range of 6 to 14 (Müller et al. 2020). It's important to note that efforts were made to establish initial feasible ranges based on estimates from other studies to avoid generating inaccurate results. The calibration process utilised observed daily and cumulative infections, as well as the death rate, with the assumption that 23% of infections occur in transit (Müller et al. 2020). For a more in-depth understanding of the calibration process, readers are referred to Najmi et al. (2021a).

To enhance the validation of the disease spread transmission model, a sensitivity analysis of the calibrated parameters is presented in Figure B1. This analysis involves running the model with a specific parameter set at its calibrated value, as well as 10% above and below that value, while keeping other parameters constant. The blue dashed line represents the base simulation, while the solid and dotted lines depict the model's response to values 10% above and below the calibrated values, respectively. Figure 7 illustrates that the base contact and infection probability per contact exhibit the highest sensitivity in the model. The incubation period and infection probability at home are the next parameters that display considerable sensitivity in the disease transmission model.

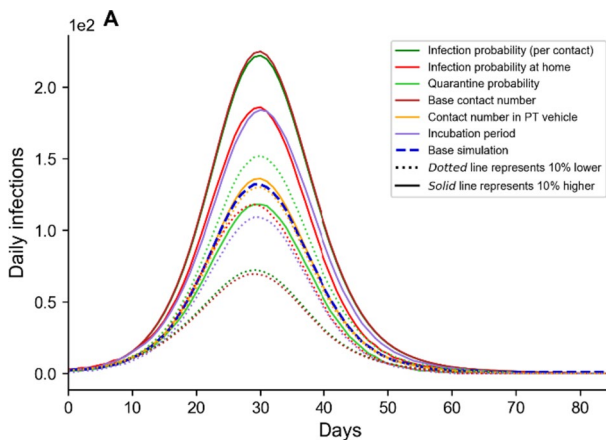


**Fig. 7** The assessment of the disease transmission model's sensitivity, measured in terms of the daily number of infections, to the calibrated parameters of the model (Najmi et al. 2021a)

**Funding** Open Access funding enabled and organized by CAUL and its Member Institutions.

## References

- Aleta, A., Martín-Corral, D., Piontti, A.P.Y., Ajelli, M., Litvinova, M., Chinazzi, M., Dean, N.E., Halloran, M.E., Longini, I.M., Merler, S., Pentland, A., Vespignani, A., Moro, E., Moreno, Y.: Modeling the impact of social distancing, testing, contact tracing and household quarantine on second-wave scenarios of the COVID-19 epidemic. *medRxiv Prepr Serv. Heal Sci.* **2020.05.06.20092841**(2020). <https://doi.org/10.1101/2020.05.06.20092841>
- Almagor, J., Picascia, S.: Exploring the effectiveness of a COVID-19 contact tracing app using an agent-based model. *Sci. Rep.* **10**, 1–11 (2020). <https://doi.org/10.1038/s41598-020-79000-y>
- Bhaskar, H.R., Mahalle, P.N., Dey, N., Santosh, K.C.: Revisited COVID-19 mortality and recovery rates: Are we missing recovery time period? *J. Med. Syst.* **44**, 1–5 (2020). <https://doi.org/10.1007/s10916-020-01668-6>
- Chang, S.L., Harding, N., Zachreson, C., Cliff, O.M., Prokopenko, M.: Modelling transmission and control of the COVID-19 pandemic in Australia. *Nat. Commun.* **11**, 1–13 (2020). <https://doi.org/10.1038/s41467-020-19393-6>
- Chang, S.L., Cliff, O.M., Zachreson, C., Prokopenko, M.: Nowcasting transmission and suppression of the Delta variant of SARS-CoV-2 in Australia (2021)
- Chu, D.K., Akl, E.A., Duda, S., Solo, K., Yaacoub, S., Schünemann, H.J., El-harakeh, A., Bognanni, A., Lotfi, T., Loeb, M., Hajizadeh, A., Bak, A., Izcovich, A., Cuello-Garcia, C.A., Chen, C., Harris, D.J., Borowiack, E., Chamseddine, F., Schünemann, F., Morgano, G.P., Muti Schünemann, G.E.U., Chen, G., Zhao, H., Neumann, I., Chan, J., Khabsa, J., Hneiny, L., Harrison, L., Smith, M., Rizk, N., Rossi, G., AbiHanna, P., El-khoury, P., Stalteri, R., Baldeh, R., Piggott, T., Zhang, T., Saad, Y., Khamis, Z., Reinap, A., M: Physical distancing, face masks, and eye protection to prevent person-to-person transmission of SARS-CoV-2 and COVID-19: a systematic review and meta-analysis. *Lancet.* **395**, 1973–1987 (2020). [https://doi.org/10.1016/S0140-6736\(20\)31142-9](https://doi.org/10.1016/S0140-6736(20)31142-9)
- Dowdle, W.R.: The principles of disease elimination and eradication. *Bull. World Health Organ.* **76**, 22–25 (1998)
- Eikenberry, S.E., Mancuso, M., Iboi, E., Phan, T., Eikenberry, K., Kuang, Y., Kostelich, E., Gumel, A.B.: To mask or not to mask: modeling the potential for face mask use by the general public to curtail the COVID-19 pandemic. *Infect. Dis. Model.* **5**, 293–308 (2020). <https://doi.org/10.1016/j.idm.2020.04.001>
- Fegert, J.M., Vitiello, B., Plener, P.L., Clemens, V.: Challenges and burden of the Coronavirus 2019 (COVID-19) pandemic for child and adolescent mental health: a narrative review to highlight clinical and research needs in the acute phase and the long return to normality. *Child. Adolesc. Psychiatry Ment Heal.* **14**, 20 (2020). <https://doi.org/10.1186/s13034-020-00329-3>
- Fisman, D.N., Tuite, A.R.: Progressive Increase in Virulence of Novel SARS-CoV-2 Variants in Ontario, Canada. *medRxiv* **2021.07.05.21260050** (2021). <https://doi.org/10.1101/2021.07.05.21260050>
- Gomez, J., Prieto, J., Leon, E., Rodríguez, A.: INFEKTA-An agent-based model for transmission of infectious diseases: the COVID-19 case in Bogotá, Colombia. *PLoS One.* **16**, e0245787 (2021). <https://doi.org/10.1371/journal.pone.0245787>
- Guan, W., Ni, Z., Hu, Y., Liang, W., Ou, C., He, J., Liu, L., Shan, H., Lei, C., Hui, D.S.C., Du, B., Li, L., Zeng, G., Yuen, K.-Y., Chen, R., Tang, C., Wang, T., Chen, P., Xiang, J., Li, S., Wang, J., Liang, Z., Peng, Y., Wei, L., Liu, Y., Peng, H.Y., Wang, P., Liu, J., Chen, J., Li, Z., Zheng, G., Qiu, Z., Luo, S., Ye, J., Zhu, C., Zhong, S., N: Clinical characteristics of Coronavirus Disease 2019 in China. *N Engl. J. Med.* **382**, 1708–1720 (2020). <https://doi.org/10.1056/nejmoa2002032>
- Hawryluck, L., Gold, W.L., Robinson, S., Pogorski, S., Galea, S., Styra, R.: SARS control and psychological effects of Quarantine, Toronto, Canada. *Emerg. Infect. Dis.* **10**, 1206 (2004). <https://doi.org/10.3201/EID1007.030703>
- Hellewell, J., Abbott, S., Gimma, A., Bosse, N.I., Jarvis, C.I., Russell, T.W., Munday, J.D., Kucharski, A.J., Edmunds, W.J., Sun, F., Flasche, S., Quilty, B.J., Davies, N., Liu, Y., Clifford, S., Klepac, P., Jit, M., Diamond, C., Gibbs, H., van Zandvoort, K., Funk, S., Eggo, R.M.: Feasibility of controlling COVID-19 outbreaks by isolation of cases and contacts. *Lancet Glob Heal.* **8**, e488–e496 (2020). [https://doi.org/10.1016/S2214-109X\(20\)30074-7](https://doi.org/10.1016/S2214-109X(20)30074-7)
- Hinch, R., Probert, W.J.M., Nurtay, A., Kendall, M., Wymant, C., Hall, M., Lythgoe, K., Bulas Cruz, A., Zhao, L., Stewart, A., Ferretti, L., Montero, D., Warren, J., Mather, N., Abueg, M., Wu, N., Legat, O., Bentley, K., Mead, T., Van-Vuuren, K., Feldner-Busztin, D., Ristori, T., Finkelstein, A., Bonsall, D.G.,

- Abeler-Dörner, L., Fraser, C.: OpenABM-Covid19-An agent-based model for non-pharmaceutical interventions against COVID-19 including contact tracing. *PLoS Comput. Biol.* **17**, e1009146 (2021). <https://doi.org/10.1371/journal.pcbi.1009146>
- Hoertel, N., Blachier, M., Blanco, C., Olfson, M., Massetti, M., Rico, M.S., Limosin, F., Leleu, H.: A stochastic agent-based model of the SARS-CoV-2 epidemic in France. *Nat. Med.* **26**, 1417–1421 (2020). <https://doi.org/10.1038/s41591-020-1001-6>
- Kemp, F., Proverbio, D., Aalto, A., Mombaerts, L., d'Hérouël, A.F., Husch, A., Ley, C., Gonçalves, J., Skupin, A., Magni, S.: Stages of COVID-19 pandemic and paths to herd immunity by vaccination: dynamical model comparing Austria, Luxembourg and Sweden. *medRxiv* 2020.12.31.20249088. (2021). <https://doi.org/10.1101/2020.12.31.20249088>
- Kirwan, R., McCullough, D., Butler, T., Perez de Heredia, F., Davies, I.G., Stewart, C.: Sarcopenia during COVID-19 lockdown restrictions: long-term health effects of short-term muscle loss. *GeroScience* 2020. **42**(42), 1547–1578 (2020). <https://doi.org/10.1007/S11357-020-00272-3>
- Kleitman, S., Fullerton, D.J., Zhang, L.M., Blanchard, M.D., Lee, J., Stankov, L., Thompson, V.: To comply or not comply? A latent profile analysis of behaviours and attitudes during the COVID-19 pandemic. *PLoS One.* **16**, e0255268 (2021). <https://doi.org/10.1371/journal.pone.0255268>
- Kucharski, A.J., Russell, T.W., Diamond, C., Liu, Y., Edmunds, J., Funk, S., Eggo, R.M., Sun, F., Jit, M., Munday, J.D., Davies, N., Gimma, A., van Zandvoort, K., Gibbs, H., Hellewell, J., Jarvis, C.I., Clifford, S., Quilty, B.J., Bosse, N.I., Abbott, S., Klepac, P., Flasche, S.: Early dynamics of transmission and control of COVID-19: a mathematical modelling study. *Lancet Infect. Dis.* **20**, 553–558 (2020). [https://doi.org/10.1016/S1473-3099\(20\)30144-4](https://doi.org/10.1016/S1473-3099(20)30144-4)
- Li, B., Deng, A., Li, K., Hu, Y., Li, Z., Xiong, Q., Liu, Z., Guo, Q., Zou, L., Zhang, H., Zhang, M., Ouyang, F., Su, J., Su, W., Xu, J., Lin, H., Sun, J., Peng, J., Jiang, H., Zhou, P., Hu, T., Luo, M., Zhang, Y., Zheng, H., Xiao, J., Liu, T., Che, R., Zeng, H., Zheng, Z., Huang, Y., Yu, J., Yi, L., Wu, J., Chen, J., Zhong, H., Deng, X., Kang, M., Pybus, O.G., Hall, M., Lythgoe, K.A., Li, Y., Yuan, J., He, J., Lu, J.: Viral infection and transmission in a large, well-traced outbreak caused by the SARS-CoV-2 Delta variant (2021). *medRxiv* 2021.07.07.21260122 <https://doi.org/10.1101/2021.07.07.21260122>
- Liu, Y., Rocklöv, J.: The reproductive number of the Delta variant of SARS-CoV-2 is far higher compared to the ancestral SARS-CoV-2 virus. *J. Travel Med.* (2021). <https://doi.org/10.1093/jtm/taab124>
- Liu, H., Zhang, J., Cai, J., Deng, X., Peng, C., Chen, X., Yang, J., Wu, Q., Chen, Z., Zheng, W., Viboud, C., Zhang, W., Ajelli, M., Yu, H.: Herd immunity induced by COVID-19 vaccination programs to suppress epidemics caused by SARS-CoV-2 wild type and variants in China. *medRxiv Prepr Serv. Heal Sci.* (2021). <https://doi.org/10.1101/2021.07.23.21261013>
- Livshits, V., Dutta, A., Maneva, P., Jeon, K., You, D., Zhu, H., Vovsha, P., Vyas, G., Hicks, J., Ory, D.: Activity-based model application for business reopening scenarios after COVID-19 (2021)
- Lopez Bernal, J., Andrews, N., Gower, C., Gallagher, E., Simmons, R., Thelwall, S., Stowe, J., Tessier, E., Groves, N., Dabrera, G., Myers, R., Campbell, C.N.J., Amirthalingam, G., Edmunds, M., Zambon, M., Brown, K.E., Hopkins, S., Chand, M., Ramsay, M.: Effectiveness of Covid-19 vaccines against the B.1.617.2 (Delta) variant. *N Engl. J. Med.* (2021). <https://doi.org/10.1056/nejmoa2108891>
- Mahdizadeh Gharakhanlou, N., Hooshangi, N.: Spatio-temporal simulation of the novel coronavirus (COVID-19) outbreak using the agent-based modeling approach (case study: Urmia, Iran). *Inf. Med. Unlocked.* **20**, 100403 (2020). <https://doi.org/10.1016/j.imu.2020.100403>
- Memorror, M.: Improving communications around vaccine breakthrough and vaccine effectiveness (2021). <https://www.cdc.gov/coronavirus>
- Miller, E.J., Roorda, M.J.: Prototype model of household activity-travel scheduling. *Transp. Res. Rec.* 114–121 (2003). <https://doi.org/10.3141/1831-13>
- Miller, E.J., Roorda, M.J., Carrasco, J.A.: A tour-based model of travel mode choice. *Transp. (Amst).* **32**, 399–422 (2005). <https://doi.org/10.1007/s11116-004-7962-3>
- Mlcochova, P., Kemp, S., Shanker Dhar, M., Papa, G., Meng, B., Mishra, S., Whittaker, C., Mellan, T., Ferreira, I., Dattir, R., Collier, D.A., Singh, S., Pandey, R., Marwal, R., Datta, M., Ponnusamy, K., Radhakrishnan, V., Abdullahi, A., Brown, J., Charles, O., Chattopadhyay, P., Devi, P., Caputo, D., Peacock, T., Wattal, C., Goel, N., Vaishya, R., Agarwal, M., Barclay, W.S., Bhatt, S., Flaxman, S., James, L., Rakshit, P., Agrawal, A., Gupta, R.K.: SARS-CoV-2 B.1.617.2 Delta variant emergence and vaccine breakthrough. (2021). <https://doi.org/10.21203/RS.3.RS-637724/V1>
- Mukerjee, S., Chow, C.M., Li, M.: Mitigation strategies and compliance in the COVID-19 fight; How much compliance is enough? *PLoS ONE.* **16**, e0239352 (2021). <https://doi.org/10.1371/JOURNAL.PONE.0239352>
- Müller, S.A., Balmer, M., Neumann, A., Nagel, K.: Mobility traces and spreading of COVID-19. *medRxiv* 1–22. (2020). <https://doi.org/10.1101/2020.03.27.20045302>

- Müller, S.A., Balmer, M., Charlton, W., Ewert, R., Neumann, A., Rakow, C., Schlenker, T., Nagel, K.: Predicting the effects of COVID-19 related interventions in urban settings by combining activity-based modelling, agent-based simulation, and mobile phone data. *PLoS One*. **16**, e0259037 (2021). <https://doi.org/10.1371/journal.pone.0259037>
- Musser, J.M., Christensen, P.A., Olsen, R.J., Long, S.W., Subedi, S., Davis, J.J., Hodjat, P., Walley, D.R., Kinsky, J.C., Gollihar, J.D.: Delta variants of SARS-CoV-2 cause significantly increased vaccine breakthrough COVID-19 cases in Houston, Texas. *medRxiv*. **2021.07.19.21260808** (2021). <https://doi.org/10.1101/2021.07.19.21260808>
- Najmi, A., Nazari, S., Safarighouzdi, F., Miller, E.J., MacIntyre, R., Rashidi, T.H.: Easing or tightening control strategies: determination of COVID-19 parameters for an agent-based model. *Transp. (Amst)*. **1–29** (2021a). <https://doi.org/10.1007/s11116-021-10210-7>
- Najmi, A., Nazari, S., Safarighouzdi, F., Raina MacIntyre, C., Miller, E.J., Rashidi, T.H.: Facemask and social distancing, pillars of opening up economies. *PLoS ONE*. **16** (2021b). <https://doi.org/10.1371/journal.pone.0249677>
- Nasreen, S., He, S., Chung, H., Brown, K.A., Gubbay, J.B., Buchan, S.A., Wilson, S.E., Sundaram, M.E., Fell, D.B., Chen, B., Calzavara, A., Austin, P.C., Schwartz, K.L., Tadrous, M., Wilson, K., Kwong, J.C., Investigators, on behalf of the C.I.R.N. (CIRN) P.C.N. (PCN): Effectiveness of COVID-19 vaccines against variants of concern, Canada. *medRxiv*. **2021.06.28.21259420v3** (2021). <https://doi.org/10.1101/2021.06.28.21259420>
- Ong, S.W.X., Chiew, C.J., Ang, L.W., Mak, T.-M., Cui, L., Toh, M.P.H., Lim, Y.D., Lee, P.H., Lee, T.H., Chia, P.Y., Maurer-Stroh, S., Lin, R.T.P., Leo, Y.-S., Lee, V.J., Lye, D.C., Young, B.E.: Clinical and virological features of SARS-CoV-2 variants of concern: a retrospective cohort study comparing B.1.1.7 (alpha), B.1.315 (Beta), and B.1.617.2 (Delta). *SSRN Electron. J.* (2021). <https://doi.org/10.2139/ssrn.3861566>
- Panovska-Griffiths, J., Stuart, R.M., Kerr, C.C., Rosenfield, K., Mistry, D., Waites, W., Klein, D.J., Bonell, C., Viner, R.M.: Modelling the impact of reopening schools in the UK in early 2021 in the presence of the alpha variant and with roll-out of vaccination against SARS-CoV-2. *medRxiv* **2021.02.07.21251287**. (2021). <https://doi.org/10.1101/2021.02.07.21251287>
- Pasaoglu, G., Harrison, G., Jones, L., Hill, A., Beudet, A., Thiel, C.: A system dynamics based market agent model simulating future powertrain technology transition: Scenarios in the EU light duty vehicle road transport sector. *Technol. Forecast. Soc. Change*. **104**, 133–146 (2016). <https://doi.org/10.1016/j.techfore.2015.11.028>
- Predominance of Delta variant among the COVID-19 vaccinated and unvaccinated individuals, India, May 2021. *J. Infect.* (2021). <https://doi.org/10.1016/J.JINF.2021.08.006>
- Roga, E.Y., Bekele, G.G., Gonfa, D.N.: Compliance level toward COVID-19 preventive measures and associated factors among the Ambo University community, 2021. *Front. Public. Heal.* **10**, 958270 (2022). <https://doi.org/10.3389/fpubh.2022.958270>
- Roorda, M.J., Carrasco, J.A., Miller, E.J.: An integrated model of vehicle transactions, activity scheduling and mode choice. *Transp. Res. Part. B Methodol.* **43**, 217–229 (2009). <https://doi.org/10.1016/j.trb.2008.05.003>
- Salvatore, M., Bhattacharyya, R., Purkayastha, S., Zimmermann, L., Ray, D., Hazra, A., Kleinsasser, M., Mellan, T., Whittaker, C., Flaxman, S., Bhatt, S., Mishra, S., Mukherjee, B.: Resurgence of SARS-CoV-2 in India: Potential role of the B.1.617.2 (Delta) variant and delayed interventions. *medRxiv*. **2021.06.23.21259405** (2021). <https://doi.org/10.1101/2021.06.23.21259405>
- Shamil, M.S., Farheen, F., Ibtehaz, N., Khan, I.M., Rahman, M.S.: An Agent-based modeling of COVID-19: Validation, analysis, and recommendations. *Cognit Comput.* **1–12** (2021). <https://doi.org/10.1007/S12559-020-09801-W/FIGURES/9>
- Sheikh, A., McMenamin, J., Taylor, B., Robertson, C.: SARS-CoV-2 Delta VOC in Scotland: demographics, risk of hospital admission, and vaccine effectiveness. *Lancet*. **397**, 2461–2462 (2021). [https://doi.org/10.1016/S0140-6736\(21\)01358-1](https://doi.org/10.1016/S0140-6736(21)01358-1)
- Silva, P.C.L., Batista, P.V.C., Lima, H.S., Alves, M.A., Guimarães, F.G., Silva, R.C.P.: COVID-ABS: an agent-based model of COVID-19 epidemic to simulate health and economic effects of social distancing interventions. *Chaos Solitons Fractals*. **139**, 110088 (2020a). <https://doi.org/10.1016/j.chaos.2020.110088>
- Silva, P.C.L., Batista, P.V.C., Lima, H.S., Alves, M.A., Guimarães, F.G., Silva, R.C.P.: COVID-ABS: an agent-based model of COVID-19 epidemic to simulate health and economic effects of social distancing interventions. *Chaos Solitons Fractals*. **139**, 110088 (2020b). <https://doi.org/10.1016/J.CHAOS.2020.110088>
- Stowe, J., Andrews, N., Gower, C., Gallagher, E., Utsi, L., Simmons, R., Thelwall, S., Tessier, E., Groves, N., Dabrera, G., Myers, R., Amirthalingam, C.C., Edmunds, G., Zambon, M., Brown, M., Hopkins,

- K., Chand, S., Ramsay, M., Lopez Bernal, M., J: Effectiveness of COVID-19 Vaccines against Hospital Admission with the Delta (B.1.617.2) Variant [WWW Document]. Public Heal. Engl. (2021). [https://doi.org/10.1016/j.idm.2020.02.001](https://khub.net/web/phe-national/public-library/-/document_library/v2WsRK3ZIEig/view_file/479607329?_com_liferay_document_library_web_portlet_DLPortlet_INSTANCE_v2WsRK3ZIEig_redirect=https%253A%252. Accessed 8 Nov 21)</a></p>
<p>Tang, B., Bragazzi, N.L., Li, Q., Tang, S., Xiao, Y., Wu, J.: An updated estimation of the risk of transmission of the novel coronavirus (2019-nCov). <i>Infect. Dis. Model.</i> <b>5</b>, 248–255 (2020). <a href=)
- Tatapudi, H., Das, T.K.: Impact of school reopening on pandemic spread: a case study using an agent-based model for COVID-19. *Infect. Dis. Model.* **6**, 839–847 (2021). <https://doi.org/10.1016/j.idm.2021.06.007>
- Tatapudi, H., Das, R., Das, T.K.: Impact assessment of full and partial stay-at-home orders, face mask usage, and contact tracing: an agent-based simulation study of COVID-19 for an urban region. *Glob Epidemiol.* **2**, 100036 (2020). <https://doi.org/10.1016/J.GLOEPI.2020.100036>
- Tatapudi, H., Das, R., Das, T.K.: Impact of vaccine prioritization strategies on mitigating COVID-19: an agent-based simulation study using an urban region in the United States. *BMC Med. Res. Methodol.* **21**, 1–14 (2021). <https://doi.org/10.1186/S12874-021-01458-9/FIGURES/8>
- Thompson, J., Wattam, S.: Estimating the impact of interventions against COVID-19: from lockdown to vaccination. *medRxiv* 1–50. (2021). <https://doi.org/10.1101/2021.03.21.21254049>
- Truszkowska, A., Behring, B., Hasanyan, J., Zino, L., Butail, S., Caroppo, E., Jiang, Z.-P., Rizzo, A., Porfiri, M.: High-resolution agent-based modeling of COVID-19 spreading in a small town. *Adv. Theory Simul.* **4**, 2000277 (2021a). <https://doi.org/10.1002/ADTS.202000277>
- Truszkowska, A., Thakore, M., Zino, L., Butail, S., Caroppo, E., Jiang, Z.-P., Rizzo, A., Porfiri, M.: Designing the safe reopening of US towns through high-resolution agent-based modeling. *Adv. Theory Simul.* (2021b). <https://doi.org/10.1002/ADTS.202100157>
- Ueki, H., Furusawa, Y., Iwatsuki-Horimoto, K., Imai, M., Kabata, H., Nishimura, H., Kawaoka, Y.: Effectiveness of face masks in preventing airborne transmission of SARS-CoV-2. *mSphere* (2020). <https://doi.org/10.1128/MSPHERE.00637-20>
- Vardavas, R., Strong, A., Bouey, J., Welburn, J., de Lima, P., Baker, L., Zhu, K., Priest, M., Hu, L., Ringel, J.: The health and economic impacts of nonpharmaceutical interventions to address COVID-19: a decision support tool for state and local policymakers. *Support Tool. State Local. Policymakers.* (2020). <https://doi.org/10.7249/tla173-1>
- Yang, W., Shaman, J.: COVID-19 pandemic dynamics in India and impact of the SARS-CoV-2 Delta (B.1.617.2) variant. *medRxiv.* 2021.06.21.21259268 (2021). <https://doi.org/10.1101/2021.06.21.21259268>

**Publisher's Note** Springer Nature remains neutral with regard to jurisdictional claims in published maps and institutional affiliations.

**Maliheh Tabasi** is a PhD candidate at the Research Centre for Integrated Transport Innovation (rCITI) at the University of New South Wales (UNSW). She holds a Master of Science degree in Transport and Highway Engineering and a Bachelor of Science in Civil Engineering from the University of Tehran (UT), Iran. Her areas of interest include travel behaviour and choice analysis, transport demand modelling and simulation, discrete choice modelling, MDCEV modelling and simulation, econometric time-use models, travel data collection, and agent-based modelling.


**Ali Najmi** is a Research Associate at the Research Centre for Integrated Transport Innovation (rCITI) at the University of New South Wales (UNSW). He holds a Ph.D. from UNSW, a Master of Science degree in Socioeconomics Engineering and a Bachelor of Science in Industrial Engineering from the Iran University of Science and Technology (IUST), Iran. His research focus on calibration of different types of transport models includes four-step models, activity-based models, market equilibrium, and super-networks.

**Eric J. Miller** is a Professor at the Department of Civil and Mineral Engineering at University of Toronto and Director of the University of Toronto Mobility Network. He is also research director at Data Management Group and Travel Modelling Group. He has Bachelor of Science and Master of Science degrees from the University of Toronto and a Ph.D. from M.I.T. His research interests include integrated land use transportation modelling, agent-based microsimulation, and sustainable transportation planning.

**C. Raina MacIntyre** is NHMRC Principal Research Fellow and Professor of Global Biosecurity. She heads the Biosecurity Program at the Kirby Institute, which conducts research in epidemiology, vaccinology, bioterrorism prevention, mathematical modelling, genetic epidemiology, and public health and clinical trials in infectious diseases. Her research falls under 4 four areas: personal protective equipment, vaccinology, epidemic response and emerging infectious diseases, and bioterrorism prevention. She is a dual-specialist physician with training in epidemiology and modelling. She is best known for research in the detailed understanding of the transmission dynamics and prevention of infectious diseases, particularly respiratory pathogens such as influenza, tuberculosis, bioterrorism agents, and vaccine-preventable infections.

**Taha H. Rashidi** is a Professor in Transport Engineering at the School of Civil and Environmental Engineering at UNSW and Director of the Research Centre for Integrated Transport Innovation (rCITI). Taha is currently leading research into the interconnectivity between travel behaviour and time use and the potential of new mobility technologies to influence this paradigm. He is also examining the capacity of social media data to complement existing data resources as part of developing an integrated multi-level modelling framework to demonstrate the relationships between land use and transport systems and the consequences this has for city planning and travel behaviour more broadly. He serves as the managing editor of the Journal of Transportation Letters and the editor of IATBR NEWS.

## Authors and Affiliations

Maliheh Tabasi<sup>1</sup> · Ali Najmi<sup>1</sup> · Eric J. Miller<sup>2</sup> · C. Raina MacIntyre<sup>3,4</sup> · Taha H. Rashidi<sup>1</sup> 

✉ Taha H. Rashidi  
rashidi@unsw.edu.au

Maliheh Tabasi  
m.tabasi@unsw.edu.au

Ali Najmi  
a.najmi@unsw.edu.au

Eric J. Miller  
eric.miller@utoronto.ca

C. Raina MacIntyre  
r.macintyre@unsw.edu.au

<sup>1</sup> Research Centre for Integrated Transport Innovation, School of Civil and Environmental Engineering, The University of New South Wales, Sydney, Australia

<sup>2</sup> Department of Civil and Mineral Engineering, University of Toronto, 35 St. George Street, Room GB305A, Toronto, Ontario M5S 1A4, Canada

<sup>3</sup> Arizona State University College of Health Solutions, Phoenix, AZ, USA

<sup>4</sup> Kirby Institute, Faculty of Medicine, The University of New South Wales, Sydney, NSW, Australia